Dalton Transactions

Cite this: *Dalton Trans.*, 2012, **41**, 5949

www.rsc.org/dalton

PAPER

Thio-Pybox and Thio-Phebox complexes of chromium, iron, cobalt and nickel and their application in ethylene and butadiene polymerisation catalysis†‡

James D. Nobbs, Atanas K. Tomov, Renan Cariou, Vernon C. Gibson, Andrew J. P. White and George J. P. Britovsek*

Received 13th February 2012, Accepted 29th February 2012
DOI: 10.1039/c2dt30324h

A series of bis(thiazolinyl)- and bis(thiazolyl)pyridine Thio-Pybox ligands and their metal complexes of chromium(III), iron(II), cobalt(II) and nickel(II) has been prepared, as well as a nickel(II) complex containing a monoanionic bis(thiazolinyl)phenyl Thio-Phebox ligand. These new metal complexes have been characterised and used as catalysts, in combination with the co-catalyst MAO, for the polymerisation of ethylene and for the polymerisation of butadiene. In the case of ethylene polymerisation, the Thio-Pybox and Thio-Phebox metal complexes have shown relatively low polymerisation activities, much lower compared to the related bis(imino)pyridine complexes of the same metals. In the polymerisation of butadiene, several Thio-Pybox cobalt(II) complexes show very high activities, significantly higher than the other metal complexes with the same ligand. It is the metal, rather than the ligand, that appears to have the most profound effect on the catalytic activity in butadiene polymerisation, unlike in the polymerisation of ethylene, where bis(imino)pyridine ligands provide highly active catalysts for a range of 1st row transition metals.

Introduction

The discovery and development of highly active olefin polymerisation catalysts is a key driver for the commercial exploitation of new polyolefinic materials as well as for improving the performance of existing polymers. An important class of non-metallocene olefin polymerisation catalysts is based on the bis(imino)pyridine ligand framework (see **I** in Fig. 1).[1–3] These ligands were initially used in combination with iron(II) and cobalt(II) salts, which upon activation with co-catalysts such as MAO gave highly active ethylene polymerisation and oligomerisation catalysts.[4–8] Subsequently, it was shown that many other metals including titanium,[9] vanadium,[9–11] and chromium[12–15] can also be supported by the bis(imino)pyridine ligand and generate active olefin polymerisation systems, although the activities are generally at least an order of magnitude lower compared to iron.

There have been many studies on the effect of catalyst performance as a function of modifications to the bis(imino)pyridine ligand framework, in particular the substituents at the imine *nitrogen* donor have been extensively investigated.[2,3] Less effort has been devoted to the effect of changes to the substituents at the imine *carbon* atom. In previous studies we have introduced substituents containing heteroatoms such as SR, OR and NR_2 at

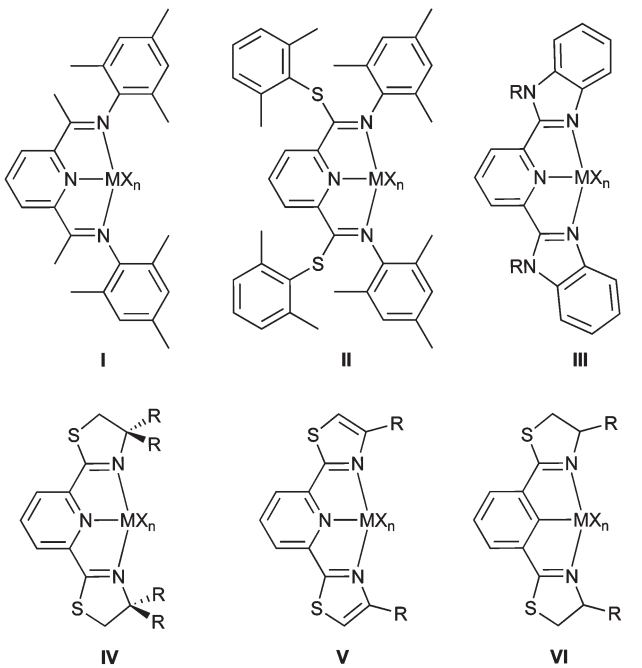

Fig. 1 Metal complexes of bis(imino)pyridine (**I** and **II**), bis(benzimidazolyl)pyridine (**III**), bis(thiazolinyl)- and bis(thiazolyl)pyridine (Thio-Pybox **IV** and **V**) and bis(thiazolinyl)phenyl ligands (Thio-Phebox **VI**).

Department of Chemistry, Imperial College London, Exhibition Road, London, SW7 2AZ, UK. E-mail: g.britovsek@imperial.ac.uk; Fax: +44-(0)20-75945804; Tel: +44-(0)20-75945863

†Dedicated to Professor David Cole-Hamilton on the occasion of his retirement and for his outstanding contribution to transition metal catalysis.

‡Electronic supplementary information (ESI) available. CCDC 859231–859239. For ESI and crystallographic data in CIF or other electronic format see DOI: 10.1039/c2dt30324h

the imine carbon and we have found that aryl-substituted SR groups such as **II** in Fig. 1, generate highly active and long-lived ethylene polymerisation catalysts based on iron, vanadium and chromium, whereas the OR-substituted complexes showed much lower activities and NR_2-substituted complexes were entirely inactive.[16,17] The use of *N*-heterocyclic groups, for example the bis(benzimidazolyl)pyridine ligands of type **III**, has also resulted in low ethylene and propylene oligomerisation activities in the case of iron.[15,18] However, other metal–ligand **III** combinations have resulted in active chromium- and nickel-based catalysts for the oligomerisation of ethylene.[19–22]

Another aspect of our research is the development of highly active catalysts for the selective polymerisation of butadiene.[23,24] Industrial interest in synthetic polybutadiene rubbers is driven by the low cost of the monomer and the wide variety and versatility of the butadiene-based polymers. Polybutadienes are formed *via* 1,4- or 1,2-insertions, which lead to *trans*-1,4, *cis*-1,4 or 1,2-vinyl microstructures, whereby the latter can be isotactic, syndiotactic or atactic. In order to gain better control over molecular weight and polymer compositions, academic and industrial research has focused in recent years on well-defined single-site catalysts, mainly based on rare earth metals and first row transition metals.[25,26] Bis(imino)pyridine ligands of type **I** have been used to prepare catalysts for the polymerisation of butadiene, using a range of first row transition metals.[27–31] We have shown previously that a bis(benzimidazolyl)pyridine cobalt(II) complex of type **III** can polymerise butadiene with a moderate activity of 70 g $mmol^{-1}$ h^{-1} to give *cis*-1,4-polybutadiene with 97% selectivity.[23]

In a further study presented here, we have prepared a series of first row transition metal complexes with thiazoline- and thiazole-based ligands **IV**, **V** and **VI** (see Fig. 1) and investigated their ability to generate active ethylene and butadiene polymerisation catalysts. These ligands, referred to as Thio-Pybox and Thio-Phebox, are sulfur-based relatives of the well known oxygen-based Pybox and Phebox ligands.[32–35] Pybox ligands have been used previously for the preparation of ethylene polymerisation catalysts based on iron(II) and ruthenium(II),[36,37] and for propylene polymerisation catalysts based on iron(II) and vanadium(III),[15] but generally very low activities have been obtained. Chromium-based Pybox complexes have been used for the polymerization of ethylene,[38] and for the selective dimerisation of ethylene to butene.[39] In addition, iron-based Pybox complexes have been applied as catalysts for aziridination reactions and for the hydrosilylation of ketones.[40,41] Only one example for the application of a Thio-Pybox ligand has been recently disclosed, where a vanadium-based catalyst with a bis(benzothiazolyl)pyridine ligand has shown a moderate activity for the polymerisation of ethylene.[42] Thio-Pybox ligands have been investigated in other areas of catalysis, for example in asymmetric cyclopropanation reactions.[43] Thio-Phebox ligands are very rare, the only examples are two late transition-metal bis(benzothiazolyl)phenyl complexes, which were obtained by a C–H activation method.[44,45]

Building on our previous success with sulfur-based substituents in the case of ligands of class **II**, we were intrigued whether first row transition metal complexes of Thio-Pybox and Thio-Phebox ligands could be prepared and would give more active olefin polymerisation catalysts compared to the analogous oxygen-based Pybox ligands. We describe here the synthesis and characterisation of a series of chromium(III), iron(II), cobalt(II) and nickel(II) complexes containing bis(thiazolinyl)pyridine ligands (**IV**) and the unsaturated bis(thiazolyl)pyridine ligands (**V**). In addition, a nickel(II) Thio-Phebox complex of type **VI**, containing the anionic bis(thiazolinyl)phenyl ligand has been prepared. The catalytic properties of these complexes for the polymerisation of ethylene and butadiene have been investigated.

Results and discussion

Ligand syntheses

The synthesis of bis(thiazolinyl)pyridine ligands has previously been carried out *via* a ring closure reaction of thioamides.[46,47] Due to the large number of steps generally required for the synthesis of the thioamides, we decided to investigate an alternative route *via* bis-(*N*-acylaminoalcohols), which can be synthesised straightforwardly from 2,6-pyridinedicarbonyl chloride and the corresponding aminoalcohol (see Scheme 1). Lawesson's reagent has been used for the ring closure of bis-(*N*-acylaminoalcohols) to give thiazolines,[48] and a similar reaction has been reported using P_2S_5 as the thiolating agent in the presence of a base.[39,47,49] By adapting these procedures, we carried out the thiolation and ring closure of a series of substituted bis-(*N*-acylaminoalcohols) using P_2S_5 in the presence of NEt_3. The reactions gave the ligands **L1–L4** in moderate yield. The absolute configuration for ligand **L1** was confirmed by X-ray crystallographic analysis (see ESI‡).

The bis(thiazolyl)pyridine ligands **L5–L7** were prepared from the corresponding α-bromoketones and 2,6-pyridine dithioamide in a modified literature procedure, based on a Hantzsch synthesis.[50] Compound **L8** was synthesised from 2-bromoisophthaloyl chloride in a two step procedure. Although only low yields were obtained (10%), this is a useful precursor to the Thio-Phebox ligand, the sulfur-based relative of the well known Phebox ligand.[35] The low yield of the reaction may be due to the insolubility of the precursor, 2-bromo-*N*,*N*′-bis[(1*R*)-2-hydroxy-1-phenylethyl]isophthalamide in refluxing toluene.

Complex synthesis

A series of complexes of the first row transition metals chromium(III), iron(II), cobalt(II) and nickel(II) containing the Thio-Pybox ligands **L1–L7** and the Thio-Phebox ligand **L8** has been prepared. All complexes were characterised by IR spectroscopy, mass spectrometry, elemental analyses, magnetic susceptibility measurements and, in selected cases, by paramagnetic NMR spectroscopy and X-ray crystallography.

Chromium complexes

Chromium complexes of ligands **L1**, **L2** and **L5** were synthesised by reacting the ligands with $CrCl_3 \cdot 3THF$ in THF or in dichloromethane for ligand **L6** (Fig. 2). The resulting air-stable green complexes were insoluble in most common organic solvents. Green crystals of complex [Cr(**L2**)Cl_3] suitable for X-ray

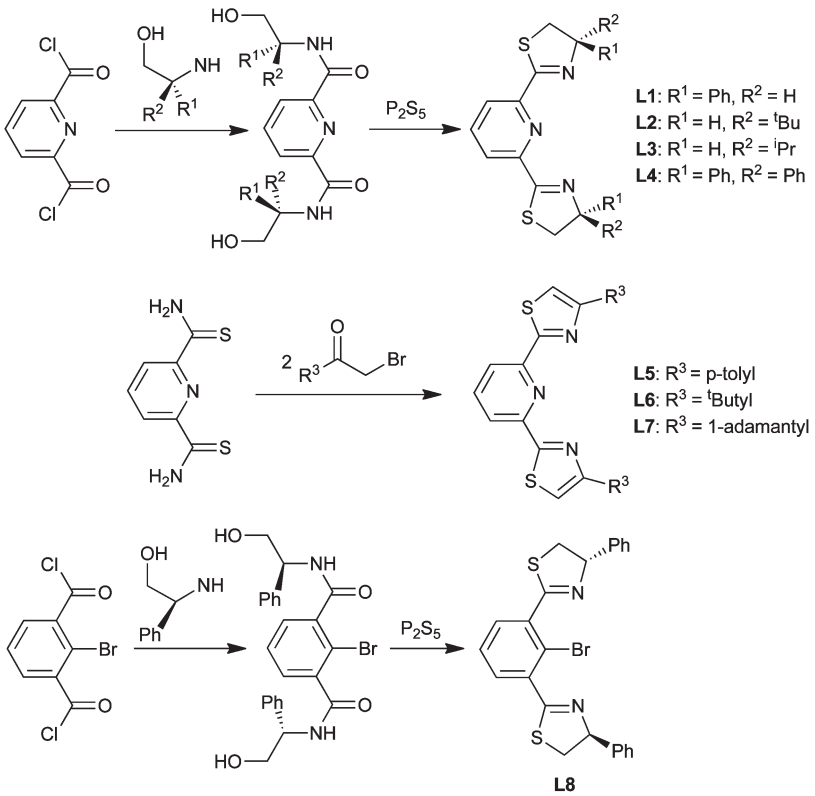

Scheme 1 Synthetic procedures for Thio-Pybox and Thio-Phebox ligands **L1**–**L8**.

diffraction were obtained from a dichloromethane–pentane solution. The molecular structure, shown in Fig. 3, shows a distorted octahedral geometry with the tridentate bis(thiazolinyl) pyridine ligand adopting a meridional coordination mode. The imine nitrogen donors, rather than the sulfur donors, bind to the chromium centre. The bond lengths and angles are similar to the bis(oxazolinyl)pyridine chromium(III) chloride complex reported previously.[38]

Iron complexes

The reaction of ligand **L1** with iron(II) chloride or iron(II) bromide in THF resulted in the formation of the bis(chelate) complexes $[Fe(\mathbf{L1})_2]^{2+}[FeX_4]^{2-}$ (X = Cl or Br). The formation of cationic bis(ligand) iron(II) complexes is common, particularly with less bulky ligands such as terpyridine or bis(benzimidazolyl)pyridine ligands of type **III** where R = H (see Fig. 1),[51,52] and has also been observed for bis(thiazolyl)pyridine ligands with small substituents (R^3 = H or Me).[53] Here, the phenyl substituents do not provide enough steric hindrance to avoid bis(chelate) formation. Single crystals of complex $[Fe(\mathbf{L1})_2][FeCl_4]$ were obtained by slowly cooling a hot saturated solution of the complex in acetonitrile. The molecular structure shows a dicationic six-coordinate iron(II) complex, balanced by an $[FeCl_4]^{2-}$ counterion in which the binding of two bis(thiazolinyl)pyridine ligands is stabilised by the presence of π–π interactions (see Fig. 4), with the pyridyl ring (**A**) of one ligand bracketed by the two phenyl rings (**B′** and **C′**) of the second C_2-related ligand, and *vice versa*.

The thiazolinyl and thiazolyl ligands **L2** and **L6**, containing *tert*-butyl substituents at the α-carbon position, react with iron(II) bromide to form a mono(chelate) complex $[Fe(\mathbf{L2})Br_2]$ and $[Fe(\mathbf{L6})Br_2]$. Single crystals of $[Fe(\mathbf{L2})Br_2]$ were obtained *via* diffusion of pentane into a solution of the complex in dichloromethane. The structure was found to contain two crystallographically independent complexes ($[Fe(\mathbf{L2})Br_2]$-I and $[Fe(\mathbf{L2})Br_2]$-II), one in a general position (I, based on Fe) and one sited about a C_2 axis (II, based on Fe′); see Fig. 5 and the ESI‡ for more details. Thiazoline and thiazole ligands are ambidentate ligands, with coordination *via* sulfur or nitrogen being both possible. However, in these cases the nitrogen donors bind to the iron(II) centre. The five-coordinate complex has a distorted square pyramidal geometry with a τ-value of 0.17 for both independent molecules. The N(1)–Fe–Br angles in $[Fe(\mathbf{L2})Br_2]$-I are similar [112.85(6) and 108.28(6)° for Br(1) and Br(2) respectively], and also similar to that in complex II [110.585(16)°] where the two angles are identical as a result of the C_2 symmetry.

Complex $[Fe(\mathbf{L2})Br_2]$ is deep blue and readily soluble in common organic solvents, whereas $[Fe(\mathbf{L6})Br_2]$ is red–brown in colour and the thiazolyl complexes are generally less soluble. The bis(chelate) iron(II) complex $[Fe(\mathbf{L1})_2][FeCl_4]$ is intensely purple, probably due to a low-spin iron(II) cation and displays much lower solubility in common organic solvents compared to $[Fe(\mathbf{L2})Br_2]$ and $[Fe(\mathbf{L6})Br_2]$. All complexes are paramagnetic ($[Fe(\mathbf{L1})_2][FeCl_4]$ due to the anion) and the paramagnetic ^{1}H NMR and COSY spectra of complex $[Fe(\mathbf{L2})Br_2]$ are shown as an example in Fig. 6 (see Experimental section for further details). The six ^{1}H NMR signals can be assigned to pyridyl protons (a = H_{para}, b = H_{meta}), methylene protons c, protons at

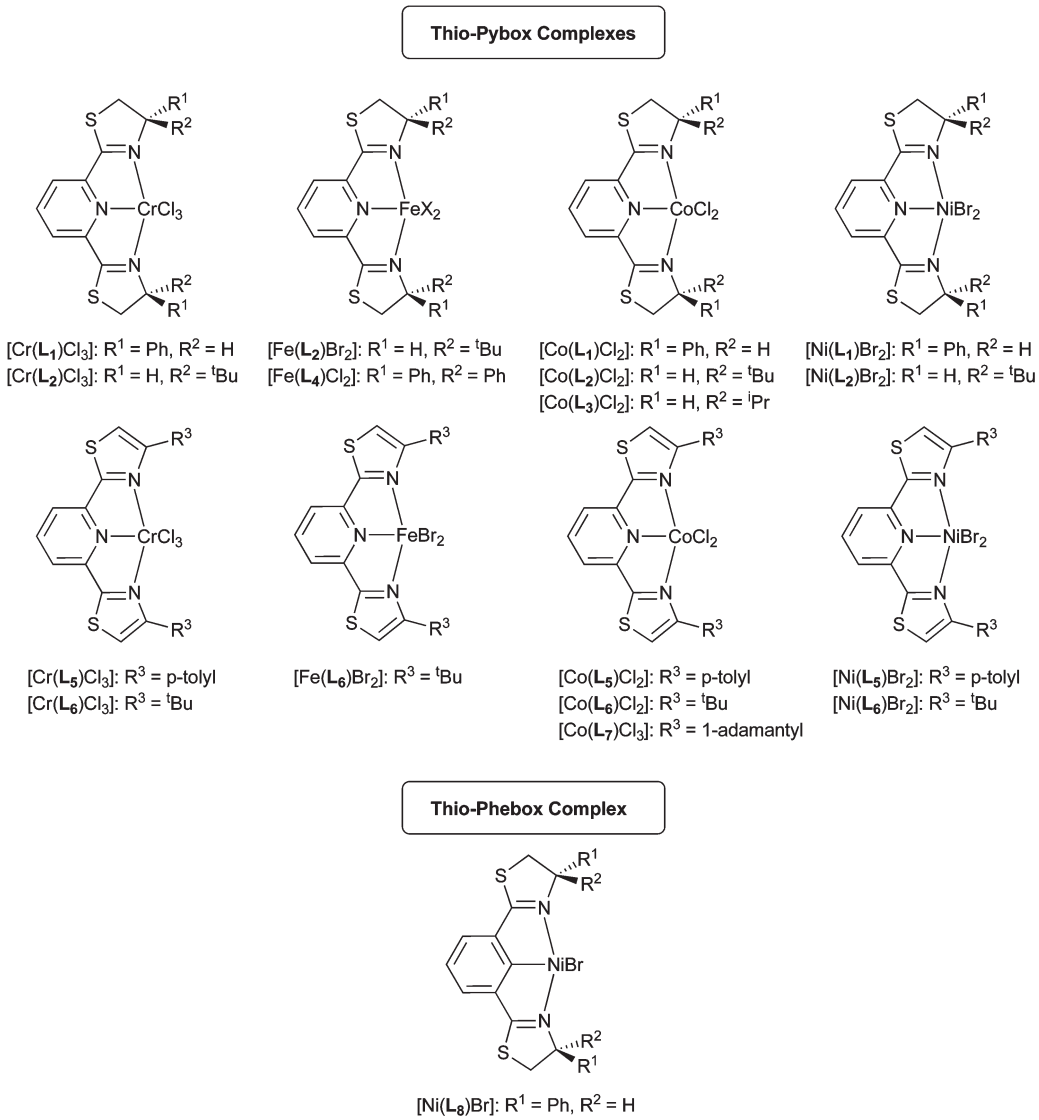

Fig. 2 Overview of Thio-Pybox and Thio-Phebox metal complexes used in this study.

the stereocentre *d* and *tert*-butyl protons *e*. Interestingly, there is a large separation in chemical shift for the pyridyl resonances *a* and *b* of 67.6 ppm. Due to their closer proximity to the iron(II) centre, the protons *d* and *e* give rise to broader signals, in comparison to the other resonances.

In an attempt to increase the steric protection around the active site, complex [Fe(**L4**)Cl_2] was prepared with thiazoline groups containing two phenyl substituents at the α-carbon. However, whereas the reactions between ligand **L2** and **L6** with iron(II) bromide in THF proceeded readily, the reaction with the sterically bulky ligand **L4** required a much longer reaction time. The reaction mixture gradually turned a characteristic intense blue colour over 48 h, indicating the formation of a metal complex. However, subsequent work-up produced low yields of the complex, which contained unidentified impurities. The complex could eventually be isolated in pure form in very low yield (<10%). A notable feature in the structure of complex [Fe(**L4**)Cl_2] is the asymmetry in the metal imine bonding (see Fig. 7). Whereas the Fe–N(7) distance of 2.2378(14) Å is typical for high spin iron(II) complexes, the Fe–N(23) bond length of 2.5923(14) Å is significantly longer, indicating a departure from the trigonal bipyramidal geometry towards a four-coordinate tetrahedral geometry.

Cobalt complexes

Bis(thiazolinyl)pyridine cobalt(II) complexes were prepared in good yield as green paramagnetic solids by reaction of the corresponding ligands **L1**–**L3** and cobalt(II) chloride in THF at room temperature. The nature of the substituents has again a significant influence on the solubility of the resulting complexes. The thiazoline complexes [Co(**L2**)Cl_2] and [Co(**L3**)Cl_2] with *tert*-butyl and iso-propyl substituents were soluble in THF whereas the phenyl-substituted complex [Co(**L1**)Cl_2] was only sparingly soluble in THF. The thiazole complexes [Co(**L5**)Cl_2], [Co(**L6**)Cl_2] and [Co(**L7**)Cl_2] were all poorly soluble in common solvents.

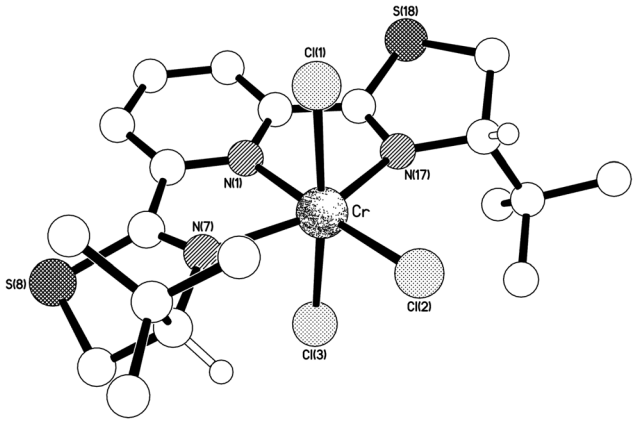

Fig. 3 The molecular structure of [Cr(**L2**)Cl_3]. Selected bond lengths (Å) and angles (°); Cr–Cl(1) 2.3259(8), Cr–Cl(2) 2.2808(7), Cr–Cl(3) 2.3181(8), Cr–N(1) 2.012(2), Cr–N(7) 2.124(2), Cr–N(17) 2.134(2), Cl(1)–Cr–Cl(2) 92.19(3), Cl(1)–Cr–Cl(3) 173.95(3), Cl(1)–Cr–N(1) 84.92(7), Cl(1)–Cr–N(7) 92.53(6), Cl(1)–Cr–N(17) 86.50(6), Cl(2)–Cr–Cl(3) 93.62(3), Cl(2)–Cr–N(1) 176.94(7), Cl(2)–Cr–N(7) 104.10(6), Cl(2)–Cr–N(17) 101.51(6), Cl(3)–Cr–N(1) 89.29(7), Cl(3)–Cr–N(7) 84.42(6), Cl(3)–Cr–N(17) 93.98(6), N(1)–Cr–N(7) 77.08(8), N(1)–Cr–N(17) 77.34(9), N(7)–Cr–N(17) 154.39(8).

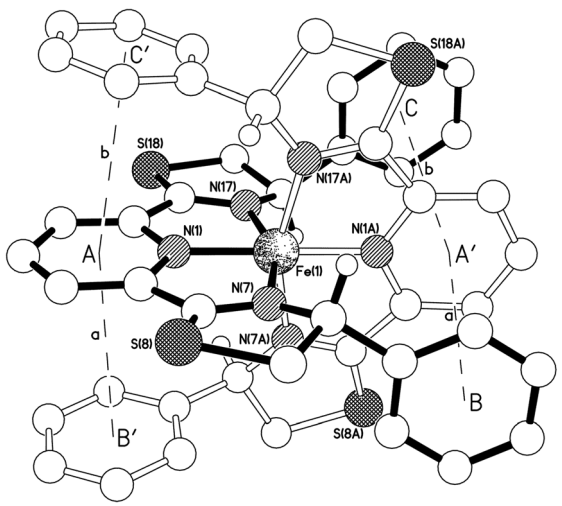

Fig. 4 The molecular structure of the C_2-symmetric $[Fe(\mathbf{L1})_2]^{2+}$ cation present in the crystals of $[Fe(\mathbf{L1})_2][FeCl_4]$. The π–π interactions **a** and **b** have centroid···centroid separations of *ca.* 3.52 and 3.67 Å respectively. Selected bond lengths (Å) and angles (°); Fe(1)–N(1) 1.888(2), Fe(1)–N(7) 1.997(2), Fe(1)–N(17) 2.003(3), N(1)–Fe(1)–N(1A) 179.97(17), N(1)–Fe(1)–N(7) 79.78(11), N(1)–Fe(1)–N(17) 79.40(11), N(1)–Fe(1)–N(7A) 100.20(11), N(1)–Fe(1)–N(17A) 100.62(11), N(7)–Fe(1)–N(17) 159.17(10), N(7)–Fe(1)–N(7A) 96.13(14), N(7)–Fe(1)–N(17A) 87.11(10), N(17)–Fe(1)–N(17A) 97.16(14).

Green single crystals of [Co(**L2**)Cl_2], [Co(**L3**)Cl_2] and [Co(**L5**)Cl_2] suitable for X-ray crystallographic analysis were obtained by the layering of a dichloromethane solution of the corresponding complex with pentane. The molecular structure for complex [Co(**L2**)Cl_2] is shown in Fig. 8 and the isostructural complex [Co(**L3**)Cl_2] in the ESI.‡ The structure of [Co(**L2**)Cl_2] was found to contain two crystallographically independent complexes ([Co(**L2**)Cl_2]-I and [Co(**L2**)Cl_2]-II), one in a general

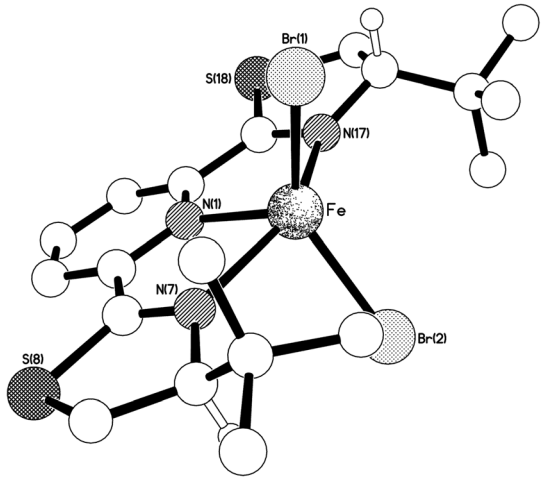

Fig. 5 The molecular structure of [Fe(**L2**)Br_2]-I, one of the two crystallographically independent complexes present in the crystals of [Fe(**L2**)Br_2]. Selected bond lengths (Å) and angles (°); Fe–Br(1) 2.4147(5), Fe–Br(2) 2.4466(5), Fe–N(1) 2.086(2), Fe–N(7) 2.362(2), Fe–N(17) 2.332(3), Br(1)–Fe–Br(2) 138.85(2), Br(1)–Fe–N(1) 112.85(6), Br(1)–Fe–N(7) 99.47(6), Br(1)–Fe–N(17) 93.43(7), Br(2)–Fe–N(1) 108.28(6), Br(2)–Fe–N(7) 89.87(5), Br(2)–Fe–N(17) 98.62(6), N(1)–Fe–N(7) 74.62(9), N(1)–Fe–N(17) 74.61(9), N(7)–Fe–N(17) 149.21(9).

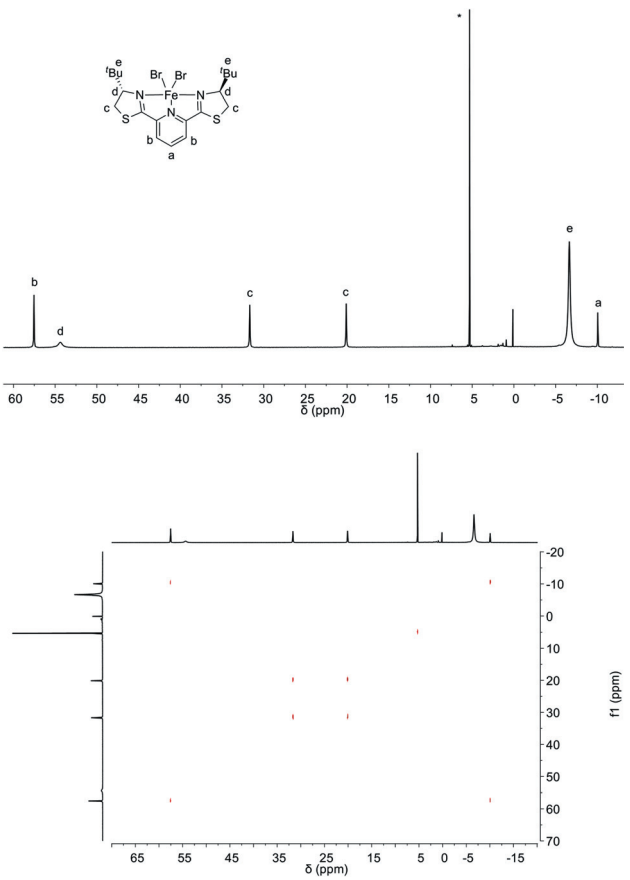

Fig. 6 Paramagnetic ^{1}H NMR spectrum and COSY spectrum of complex [Fe(**L2**)Br_2] in CD_2Cl_2 (*) at 298 K.

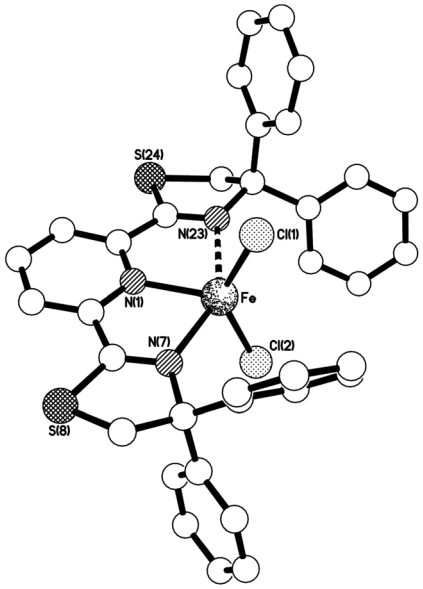

Fig. 7 The molecular structure of [Fe(**L4**)Cl_2]. Selected bond lengths (Å) and angles (°); Fe–Cl(1) 2.2310(5), Fe–Cl(2) 2.2730(5), Fe–N(1) 2.0937(14), Fe–N(7) 2.2378(14), Fe–N(23) 2.5923(14), Cl(1)–Fe–Cl(2) 135.93(2), Cl(1)–Fe–N(1) 114.62(4), Cl(1)–Fe–N(7) 100.97(4), Cl(1)–Fe–N(23) 93.39(3), Cl(2)–Fe–N(1) 108.80(4), Cl(2)–Fe–N(7) 95.69(4), Cl(2)–Fe–N(23) 93.23(3), N(1)–Fe–N(7) 76.81(5), N(1)–Fe–N(23) 71.52(5), N(7)–Fe–N(23) 148.30(5).

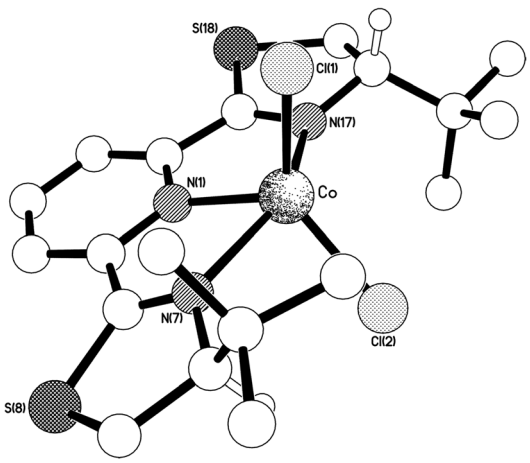

Fig. 8 The molecular structure of [Co(**L2**)Cl_2]-I, one of the two crystallographically independent complexes present in the crystals of [Co(**L2**)Cl_2]. Selected bond lengths (Å) and angles (°); Co–Cl(1) 2.2717(8), Co–Cl(2) 2.2518(8), Co–N(1) 2.034(2), Co–N(7) 2.353(2), Co–N(17) 2.256(2), Cl(1)–Co–Cl(2) 128.90(3), Cl(1)–Co–N(1) 109.30(7), Cl(1)–Co–N(7) 98.86(6), Cl(1)–Co–N(17)) 93.35(6), Cl(2)–Co–N(1) 120.94(7), Cl(2)–Co–N(7) 86.73(6), Cl(2)–Co–N(17) 106.02(6), N(1)–Co–N(7) 74.27(8), N(1)–Co–N(17) 76.59(8), N(7)–Co–N(17) 150.71(8).

position (based on Co) and one sited about a C_2 axis (based on Co′, see the ESI‡). In contrast to the pattern of similarity seen for the two independent complexes of the $FeBr_2$ analogue, here the N(1)–Co–Cl angles in complex I differ markedly from each other [109.30(7) and 120.94(7)° for Cl(1) and Cl(2) respectively], and from that in complex II [117.14(2)°] where the two

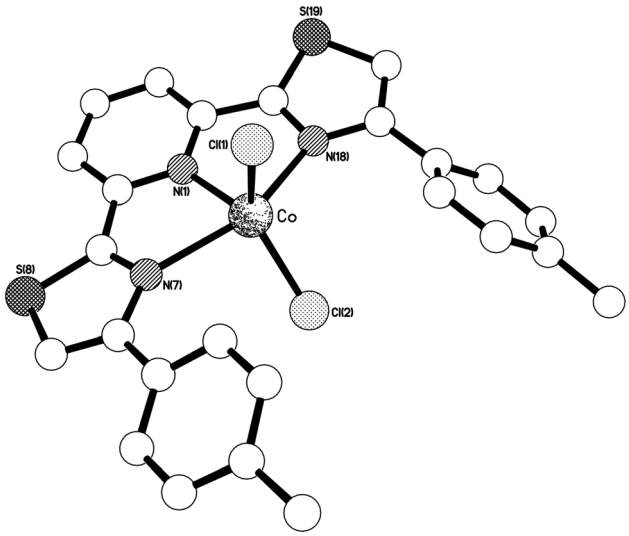

Fig. 9 The molecular structure of [Co(**L5**)Cl_2]. Selected bond lengths (Å) and angles (°); Co–Cl(1) 2.2844(5), Co–Cl(2) 2.2409(5), Co–N(1) 2.0351(14), Co–N(7) 2.3036(14), Co–N(18) 2.2224(15), Cl(1)–Co–Cl(2) 130.51(2), Cl(1)–Co–N(1) 105.04(5), Cl(1)–Co–N(7) 97.45(4), Cl(1)–Co–N(18) 92.50(4), Cl(2)–Co–N(1) 124.46(5), Cl(2)–Co–N(7) 94.23(4), Cl(2)–Co–N(18) 98.44(4), N(1)–Co–N(7) 76.20(5), N(1)–Co–N(18) 76.72(6), N(7)–Co–N(18) 152.75(5).

angles are identical as a result of the C_2 symmetry. This difference between the two independent molecules can be viewed as a rotation of the $CoCl_2$ unit with respect to the N(7)···N(17) vector, and would be expected to have an effect on the square pyramidal/trigonal bipyramidal nature of the metal centre. The geometries of the $CoCl_2$ unit in complexes I and II are similar, the Co–Cl bond lengths ranging between 2.2502(7) and 2.2717(8) Å, with Cl–Co–Cl angles of 128.90(3) and 125.73(5)° respectively. However, as the apical atom in each case is the pyridyl nitrogen N(1) and it is the N(1)–Co–Cl angles that have changed, this rotation has almost no effect on the τ parameter (0.36 and 0.40 in complexes I and II respectively).

Complex [Co(**L5**)Cl_2] adopts a distorted square pyramidal structure with a τ value of 0.37 (Fig. 9). The bond lengths in the five-membered heterocycles of the ligand reflect the aromatic character of the thiazole rings. While the Co–N(py) bond length of 2.0351(14) Å is typical, the Co–N(thiazole) bond lengths are noticeably different from one another. The Co–N(18) bond length of 2.2224(15) Å is shorter than the Co–N(7) bond length of 2.3036(14) Å, suggesting a similar but less pronounced distortion as seen in complex [Fe(**L4**)Cl_2] (Fig. 7).

Nickel complexes

Nickel(II) complexes have been synthesised by the reaction of nickel(II) bromide with the ligands **L1**, **L2**, **L5** and **L6** in THF. Complexes [Ni(**L1**)Br_2], [Ni(**L2**)Br_2] and [Ni(**L5**)Br_2] were obtained in high yield as air-stable yellow solids, whilst complex [Ni(**L6**)Br_2] was isolated as a peach coloured solid in moderate yield. The Thio-Phebox complex [Ni(**L8**)Br] was synthesised *via* an oxidative addition reaction of the ligand precursor **L8** with bis(cyclooctadiene)nickel(0), yielding an orange solid in good yield (79%). The diamagnetic, square planar, nickel(II)

complex [Ni(**L8**)Br] was analysed by ^{1}H and ^{13}C NMR spectroscopy, X-ray crystallography, mass spectrometry, IR spectroscopy and elemental analysis. The molecular structure is depicted in Fig. 10. The complex possesses a distorted square planar geometry, the metal and the four donor atoms being coplanar to better than 0.01 Å and the C–phenyl bonds are inclined by *ca*. 68° to this plane.

Ethylene polymerisation studies

The catalytic properties of the various metal complexes synthesised in this study for the polymerisation of ethylene has been investigated using methylaluminoxane (MAO) as the co-catalyst (see Experimental section for details). The chromium(III) complexes [Cr(**L1**)Cl_3], [Cr(**L2**)Cl_3], [Cr(**L5**)Cl_3] and [Cr(**L6**)Cl_3] gave a moderate ethylene polymerisation activity of 10–50 g $mmol^{-1}$ h^{-1} bar^{-1}. In addition to solid polyethylene, all chromium catalysts produced small amounts of soluble low molecular weight polyethylene with a Schulz–Flory distribution, as shown by GC analysis. These ethylene polymerisation activities are slightly better, but overall comparable, to those obtained previously with related Pybox chromium complexes.[38]

The addition of MAO to a solution of complex [Fe(**L1**)$_2$][$FeCl_4$] in toluene results in no visible colour change and no ethylene polymerisation was observed. The addition of MAO to [Fe(**L2**)Br_2] in toluene produces a colour change from deep blue to yellow, which is similar to the colour change observed upon the addition of MAO to the standard bis(imino)pyridine iron(II) chloride complex of type **I** (Fig. 1). Despite this similar change in colour upon MAO addition, the iron(II) complex [Fe(**L2**)Br_2] does not catalyse the polymerisation of ethylene under the conditions used. These results are comparable to the very low polymerisation activities reported for the related Pybox iron complexes.[36]

The cobalt-based catalysts containing ligands **L1–L3** and **L5–L7** were generally less active than the chromium catalysts under these conditions, typically 5–10 g $mmol^{-1}$ h^{-1} bar^{-1} and produced an oligomer distribution with significant isomerisation in each fraction (see for example the GC trace in Fig. S18‡ for [Co(**L2**)Cl_2]).

The Thio-Pybox nickel(II) complexes [Ni(**L1**)Br_2], [Ni(**L2**)Br_2] and [Ni(**L5**)Br_2] as well as the Thio-Phebox complex [Ni(**L8**)Br_2] were all found to be inactive for the polymerisation of ethylene under these conditions. However, complex [Ni(**L6**)Br_2] did show some dimerisation activity for the formation of butene.

We can therefore safely conclude that the introduction of sulfur-based substituents as in the range of Thio-Pybox ligands studied here, does not offer any significant improvement in terms of ethylene polymerisation activity in the case of chromium-, iron-, cobalt- and nickel-based catalysts, under the conditions used here. We therefore decided to investigate the catalytic activity of these complexes for other olefins, in particular butadiene.

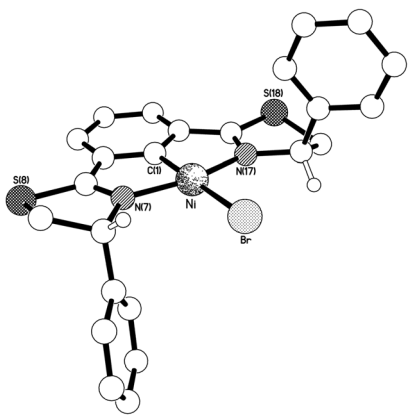

Fig. 10 The molecular structure of the Thio-Phebox complex [Ni(**L8**)Br]. Selected bond lengths (Å) and angles (°); Ni–Br 2.3548(3), Ni–C(1) 1.8371(19), Ni–N(7) 1.9217(18), Ni–N(17) 1.9193(17), Br–Ni–C(1) 179.87(7), Br–Ni–N(7) 98.75(5), Br–Ni–N(17) 98.57(5), C(1)–Ni–N(7) 81.35(8), C(1)–Ni–N(17) 81.32(8), N(7)–Ni–N(17) 162.67(8).

Butadiene polymerisation studies

The catalytic activity of the series of Thio-Pybox metal complexes in the polymerisation of butadiene was investigated under a range of reaction conditions. Determining correlations between metal and ligand effects in butadiene polymerisation has proven difficult in previous studies.[23] We started our systematic investigation with a series of complexes containing the same ligand under identical reaction conditions, but with different metals: [Cr(**L2**)Cl_3], [Fe(**L2**)Br_2], [Co(**L2**)Cl_2] and [Ni(**L2**)Br_2]. The polymerisation results including the molecular weights and polydispersity indices for the polymers obtained with the different catalysts are collected in Table 1.

It can be seen from Table 1 that the type of metal has a significant effect on the polymerisation activity and the resulting polymer properties. The activity of the complexes varies by several orders of magnitude, with very low activity exhibited by the chromium complex [Cr(**L2**)Cl_3] to intermediate activities

Table 1 Polymerisation of butadiene using different metal catalysts [M(**L2**)X_n]

							Microstruct. (%)		
Catalyst (μmol)	Time (min)	Yield (g)	Activity (g $mmol^{-1}$ h^{-1})	M_n	M_w	PDI	*cis*	*trans*	*vinyl*
[Cr(**L2**)Cl_3] (10)	30	0.01	2	nd	nd	nd	>99	0	0
[Fe(**L2**)Br_2] (10)	30	4.40	880	110 000	194 000	1.77	73	17	10
[Co(**L2**)Cl_2] (2)	10	0.94	2820	840 000	1 315 000	1.57	>99	0	0
[Ni(**L2**)Br_2] (10)	30	2.84	570	18 000	88 000	4.96	94	4	2

Conditions: MAO (500 eq.), RT, toluene (20 mL), catalyst solution stirred under 1 bar butadiene pressure for 15 minutes prior to activation and the pressure maintained during the polymerisation. M_n and M_w determined by GPC in chloroform against polystyrene standards.

with the iron and nickel complexes. Very high activity was observed in the case of the cobalt complex [Co(**L2**)Cl_2], such that the amount of catalyst and the reaction time had to be reduced significantly. These activities are much higher than those observed previously using bis(benzimidazolyl)pyridine cobalt catalysts of type **III** (Fig. 1) and related bis(benzimidazolyl)methylamine cobalt complexes, as well as $CoCl_2$, which showed an activity of 480 g $mmol^{-1}$ h^{-1} under comparable reaction conditions.[23]

The rather low activity in the case of the chromium catalyst [Cr(**L2**)Cl_3] is surprising considering that much higher activities have been observed with a bis(benzimidazolyl)methylamine chromium catalyst,[24] which incidentally produced polybutadiene with a *trans*-1,4-microstructure. This indicates that the ligand can have a significant influence on the polymerisation activity and the microstructure of the resulting polymer in the case of chromium. The other thiazolinyl complex [Cr(**L1**)Cl_3] gave a similarly low activity of 13 g $mmol^{-1}$ h^{-1} after 60 min, whereas the thiazolyl complexes [Cr(**L5**)Cl_3] and [Cr(**L6**)Cl_3] were completely inactive. A dramatic decrease in activity was also observed in the case of iron where the polymerisation activity changed from 880 to 20 g $mmol^{-1}$ h^{-1} under the same conditions, by changing the catalyst from the thiazolinyl complex [Fe(**L2**)Br_2] to the sterically almost identical thiazolyl complex [Fe(**L6**)Br_2]. Similarly in the case of cobalt, the catalytic activity decreased from 2820 to 790 g $mmol^{-1}$ h^{-1} on changing the catalyst from [Co(**L2**)Cl_2] to [Co(**L6**)Cl_2]. These results appear to suggest that the unsaturated thiazolyl substituents are generally less active compared to the saturated thiazolinyl complexes. However, the cobalt complex [Co(**L5**)Cl_2] containing the *para*-tolyl substituent shows a much higher catalytic activity of 3790 g $mmol^{-1}$ h^{-1} under the same conditions. This particular ligand **L5** also gave a higher activity in the case of nickel, resulting in 880 g $mmol^{-1}$ h^{-1} for [Ni(**L5**)Cl_2] compared to 570 g $mmol^{-1}$ h^{-1} for [Ni(**L2**)Cl_2] under the same conditions. These results illustrate once again that correlating catalytic activity in butadiene polymerisation with ligand or metal complex structure is not straightforward. However, these results do show that cobalt provides the most active butadiene polymerisation catalysts. Unlike in the polymerisation of ethylene, the metal appears to have the most profound effect on the catalytic activity in butadiene polymerisation. There are subtle ligand effects discernable but they are not easily rationalised at this stage.

The microstructure of the resulting polymers was significantly affected by the choice of metal. The highly active cobalt complex [Co(**L2**)Cl_2] was also highly selective towards *cis* polybutadiene which is the polymer of most commercial significance. The polybutadiene was of very high molecular weight (M_w = 1 315 000 g mol^{-1}) and had a narrow polydispersity index of 1.57. The polybutadiene produced by the iron and nickel complexes contained a mixture of *cis*, *trans* and *vinyl* polybutadiene. In the case of the chromium complex [Cr(**L2**)Cl_3], insufficient polymer was obtained to enable molecular weight characterisation.

Conclusions

A series of novel transition metal complexes containing Thio-Pybox and Thio-Phebox ligands have been synthesised and characterised. Their catalytic properties in the polymerisation of ethylene have been investigated, using MAO as the co-catalyst. The iron and nickel complexes tested were found to be inactive, whereas low ethylene polymerisation activities were achieved with the cobalt and chromium Thio-Pybox complexes. It is interesting to note that bis(imino)pyridine ligands with sulfur-based substituents (type **II**, Fig. 1) have shown very high polymerisation activities for a range of transition metals, including chromium, vanadium, iron and cobalt. In contrast, the ethylene polymerisation studies carried out here have shown that the Thio-Pybox ligands do not offer any advantage in terms of ethylene polymerisation activity compared to the previously investigated Pybox complexes. The special properties of the bis(imino)pyridine ligands **I** and **II** to generate highly active ethylene polymerisation catalysts for a range of metals, in particular iron, remain to be fully understood.

The Thio-Pybox complexes were also applied as catalysts for the polymerisation of butadiene. The effect of the metal upon activity and polymer properties was found to be significant, perhaps more so than the effect of the ligand. The cobalt complexes were found to be extremely active, with the highest activity of 3790 g $mmol^{-1}$ h^{-1} being observed for complex [Co(**L5**)Cl_2]. The iron and nickel Thio-Pybox complexes displayed intermediate activities, whereas the chromium complexes showed disappointingly low activities. The polymer microstructure was found to be primarily dependent upon the metal, with the cobalt and chromium complexes giving highly selective *cis*-polybutadiene and the nickel and iron complexes providing of a mixture of *cis*-, *trans*-, and *vinyl*-polybutadiene.

Experimental

Air and moisture sensitive reactions were carried out using standard Schlenk techniques under an atmosphere of purified nitrogen. Air and moisture sensitive compounds were stored in a nitrogen filled glove-box at room temperature. ^1H and ^{13}C NMR data were recorded on 400 MHz or 500 MHz Bruker spectrometers and were referenced internally to the residual ^1H and ^{13}C NMR signal of the deuterated solvents. IR spectra were recorded on a Perkin-Elmer 1760X FT-IR spectrometer using KBr discs. Mass spectra were recorded on a Micromass Autospec Q Spectrometer using electrospray ionisation (ESI). Elemental analyses were carried out by the London Metropolitan University. Oligomers were analysed *via* gas chromatography using an Agilent 6890 series GC equipped with a SGE BPX-5 capillary column (5% diphenyl 95% dimethylpolysilphenylene–siloxane, 60 m × 0.32 mm). Polybutadiene samples soluble in chloroform were analysed using Cirrus GPC/SEC software, connected to a Shodex RI-101 detector versus polystyrene standards (molecular weight 580–7 500 000). Samples were injected onto two linear 10 micron columns, using chloroform as eluant, at a flow rate of 1.0 cm^3 min^{-1} at 35 °C.

Solvents and reagents

Heptane, pentane and toluene were dried by passing through a cylinder filled with commercially available Q-5 reactant and Al_2O_3 under a pressure of nitrogen. Dichloromethane and

acetonitrile were dried by heating at reflux temperature over calcium hydride. Diethyl ether and tetrahydrofuran were dried in a similar manner by heating at reflux temperature over sodium benzophenone ketyl. All solvents were degassed prior to use. All NMR solvents, CD_2Cl_2, $CDCl_3$ and C_6D_6 were dried and stored over molecular sieves (4 Å). The following precursors were synthesised according to published procedures or modifications thereof: chromium(III) chloride tetrahydrofuran complex,[54] 2-bromoisophthalic acid,[55] pyridine-2,6-dithioamide,[56] 2-diphenylglycinol.[57] Pyridine-2,6-dicarbonyldichloride, (*R*)-(−)-2-amino-2-phenylethanol, L-valinol, (*S*)-*tert*-leucinol, 1-bromopinacalone, 1-adamantyl bromomethylketone, 2-bromo-4′-methylacetophenone and bis(1,5-cyclooctadiene)nickel(0) were obtained from commercial sources. 1,3-Butadiene and MAO were purchased from Aldrich and used without further purification. Ethylene (CP grade) was purified by passing it through an Oxy-trap and gas drier (Alltech Associates).

N,*N*′-Bis[(1*R*)-2-hydroxy-1-phenylethyl]pyridine-2,6-dicarboxamide

A solution of 2,6-pyridinedicarbonyl dichloride (3.98 g, 19.5 mmol) in dry DCM (100 mL) was added dropwise to a mixture of (*R*)-(−)-2-amino-2-phenylethanol (5.5 g, 40.1 mmol) and triethylamine (4.06 g, 40.1 mmol) in dry DCM (150 mL). After the addition, the reaction mixture was heated at reflux temperature for 12 h. Upon cooling the solution was washed with water (5 × 50 mL). The organic layer was separated, dried over sodium sulfate and then evaporated to yield a white solid. Yield = 5.9 g (75%). ^{1}H NMR ($CDCl_3$, 400 MHz): 8.61 (2H, d, *J* 7.3 Hz, N*H*), 8.33 (2H, d, *J* 7.8 Hz, Ar*H*), 8.04 (1H, t, *J* 7.8 Hz, Ar*H*), 7.42–7.31 (10H, m, Ar*H*), 5.28–5.24 (2H, m, C*H*) and 4.02 (4H, d, *J* 4.8 Hz, CH_2). ^{13}C NMR ($CDCl_3$, 101 MHz): 163.6, 148.5, 139.3, 138.8, 129.0, 128.0, 126.7, 125.2, 66.5 and 55.9. IR (KBr, cm^{-1}): 3305 (s), 2934 (w), 2877 (w), 1660 (s), 1604 (w), 1586 (w), 1532 (s), 1495 (w), 1445 (m), 1401 (w), 1357 (w), 1313 (w), 1242 (w), 1193 (w), 1167 (w), 1074 (m), 1039 (m), 999 (w), 946 (w), 913 (w), 842 (m), 753 (m), 700 (s), 646 (w), 564 (w), 524 (w) and 425 (w). MS (ESI): *m*/*z* 428 (50%) and 406 (M^+, 100%). Elem. Anal. Calcd for $C_{23}H_{23}N_3O_4$: C, 68.13; H, 5.72; N, 10.36. Found: C, 68.07; H, 5.64; N, 10.26.

N,*N*′-Bis[(1*S*)-1-(hydroxymethyl)-2-*tert*-butyl]pyridine-2,6-dicarboxamide

Prepared according to the procedure for **1** using pyridine-2,6-dicarbonyldichloride (1.30 g, 6.38 mmol), DCM (70 mL), (*S*)-*tert*-leucinol (1.49 g, 12.7 mmol) and triethylamine (1.29 g, 12.7 mmol) in DCM (50 mL). Yield = 1.54 g (66%). ^{1}H NMR ($CDCl_3$, 400 MHz): 8.31 (2H, d, *J* 7.8 Hz, Ar*H*), 8.09 (2H, d, *J* 9.3 Hz, N*H*), 8.03 (1H, t, *J* 7.8 Hz, Ar*H*), 4.03–3.95 (4H, m, CH_2), 3.79–3.72 (2H, m, NC*H*), 2.82 (2H, s, OH), 1.07 (18H, s, *t*-Bu). ^{13}C NMR ($CDCl_3$, 101 MHz): 164.3, 148.6, 139.3, 125.2, 63.1, 59.9, 34.0 and 27.0. IR (KBr, cm^{-1}): 3399 (s), 2965 (s), 1670 (s), 1534 (s), 1476 (w), 1445 (w), 1399 (m), 1367 (w), 1234 (m), 1174 (m), 1083 (w), 1052 (m), 1021 (w), 1000 (m), 843 (m), 754 (m), 680 (w) and 645 (w). MS (ESI): *m*/*z* 388 (100%, M + Na) and 366 (35%, M + H). Elem. Anal. Calcd for $C_{19}H_{31}N_3O_4$: C, 62.44; H, 8.55; N, 11.50. Found: C, 62.51; H, 8.45; N, 11.44.

N,*N*′-Bis[(1*S*)-1-(hydroxymethyl)-2-methylpropyl]pyridine-2,6-dicarboxamide

Prepared according to the procedure for **1** using pyridine-2,6-dicarbonyldichloride (3.79 g, 18.6 mmol), DCM (120 mL), L-valinol (3.83 g, 37.1 mmol) and triethylamine (3.76 g, 37.1 mmol). Yield = 5.74 g (91%). ^{1}H NMR ($CDCl_3$, 400 MHz): 8.35 (2H, d, *J* 7.8 Hz, Ar*H*), 8.01 (1H, t, *J* 7.8 Hz, Ar*H*), 8.05 (2H, d, *J* 9.0 Hz, N*H*), 4.00–3.93 (2H, m, NC*H*), 3.90–3.82 (4H, m, CH_2), 2.35 (2H, s, O*H*), 2.14–2.05 (2H, m, C*H*(CH_3)$_2$), 1.07 (6H, d, *J* 7.0 Hz, CHCH_3) and 1.05 (6H, d, *J* 7.0 Hz, CHCH_3). ^{13}C NMR ($CDCl_3$, 101 MHz): 164.1, 148.7, 139.3, 125.1, 63.9, 57.2, 29.3, 19.7 and 18.6. IR (KBr, cm^{-1}): 3425 (s), 3291 (s), 2964 (m), 2875 (w), 2605 (w), 2498 (w), 1656 (s), 1543 (s), 1462 (m), 1447 (m), 1389 (m), 1371 (m), 1327 (w), 1240 (w), 1219 (w), 1171 (w), 1125 (w), 1091 (w), 1073 (m), 1054 (m), 997 (m), 983 (w), 930 (w), 850 (m), 753 (m), 698 (m), 646 (m), 621 (w), 553 (w) and 534 (w). MS (ESI): *m*/*z* 360 (M + Na) and 338 (M + H). Elem. Anal. Calcd for $C_{17}H_{27}N_3O_4$: C, 60.51; H, 8.07; N, 12.45. Found: C, 57.15; H, 8.60; N, 12.38.

N,*N*′-Bis(2-hydroxy-1,1-diphenylethyl)pyridine-2,6-carboxamide

Prepared according to the procedure for **1** using pyridine-2,6-dicarbonyldichloride (1.91 g, 18.6 mmol), DCM (120 mL), 2,2-diphenylglycinol (4.00 g, 18.75 mmol) and triethylamine (1.99 g, 19.67 mmol). Yield = 2.70 g (52%). ^{1}H NMR ($CDCl_3$, 400 MHz): 8.80 (2H, s, N*H*), 8.42 (2H, d, $^3J_{HH}$ = 7.8 Hz, Ar*H*), 8.13 91H, t, $^3J_{HH}$ = 7.8 Hz, Ar*H*), 7.27 (20H, m, Ar*H*) and 4.45 (4H, s, –CH_2–). ^{13}C NMR ($CDCl_3$, 101 MHz): 163.2, 148.7, 141.8, 139.8, 128.6, 127.8, 127.3, 125.6, 69.4 and 68.4. IR (KBr, cm^{-1}): 3276 (m), 3059 (w), 3025 (w), 2900 (w), 2850 (m), 1683 (m), 1652 (s), 1600 (w), 1582 (w), 1568 (w), 1527 (s), 1493 (s), 1464 (w), 1445 (s), 1348 (w), 1313 (w), 1288 (w), 1248 (m), 1182 (w), 1143 (w), 1109 (m), 1078 (m), 1061 (w), 1046 (w), 1027 (w), 1000 (m), 916 (w), 841 (m), 793 (s), 754 (s), 698 (s), 636 (m), 600 (m), 587 (w), 569 (w) and 529 (w). MS (ESI): *m*/*z* 558 ([M + H]$^+$, 50%). Elem. Anal. Calcd for $C_{35}H_{31}N_3O_4$: C, 75.38; H, 5.60; N, 7.54. Found: C, 75.42; H, 5.58; N, 7.45.

2-Bromo-*N*,*N*′-bis[(1*R*)-2-hydroxy-1-phenylethyl]isophthalamide

Prepared according to the procedure for **1** using 2-bromoisophthaloyl dichloride (3.87 g, 13.73 mmol), (*R*)-(−)-2-amino-phenylethanol (3.77 g, 27.48 mmol) and triethylamine (2.92 g, 28.86 mmol) in dry DCM (50 mL). Yield = 5.55 g (83%). ^{1}H NMR (d$_6$-DMSO, 400 MHz): 8.86 (2H, d, $^3J_{HH}$ = 8.3 Hz, N*H*), 7.51–7.23 (13H, m, Ar*H*), 5.02 (2H, q, $^3J_{HH}$ = 6.9 Hz, NC*H*), 4.91 (2H, t, $^3J_{HH}$ = 5.8 Hz, O*H*), and 3.69–3.60 (4H, m, CH_2). ^{13}C NMR (d$_6$-DMSO, 101 MHz): 167.3, 141.3, 140.7, 129.3, 128.5, 127.8, 127.6, 127.3, 116.6, 65.1 and 56.1. IR (KBr, cm^{-1}): 3280 (s), 3064 (w), 2944 (w), 2878 (w), 1652 (s), 1590 (w), 1541 (m), 1494 (w), 1451 (w), 1401 (w), 1360 (w), 1305 (m), 1271 (w), 1222 (w), 1200 (w), 1118 (w), 1068 (w), 1041

(m), 1030 (m), 909 (w), 877 (w), 850 (w), 802 (w), 745 (m), 722 (m), 698 (s), 627 (w) and 530 (w).

MS (ESI): *m/z* 483 ($[M + H]^+$, 100%). Elem. Anal. Calcd for $C_{24}H_{23}BrN_2O_4$: C, 59.64; H, 4.80; N, 5.80. Found: C, 59.71; H, 4.71; N, 5.69.

2,6-Bis[(4*R*)-4-phenyl-4,5-dihydro-1,3-thiazol-2-yl]pyridine, L1

Triethylamine (6.2 g, 61.3 mmol) was added to a mixture of *N*,*N*′-bis[(1*R*)-2-hydroxy-1-phenylethyl]pyridine-2,6-dicarboxamide (0.50 g, 1.23 mmol) and phosphorus pentasulfide (0.83 g, 3.68 mmol) in dry toluene (80 mL). The mixture was heated to reflux temperature and stirred for approximately 3 h. After the mixture had cooled, water was added (20 mL) and the organic layer separated and dried over sodium sulfate. Removal of the solvent and recrystallisation from methanol gave a yellow solid. Yield = 0.15 g (30.4%). ^{1}H NMR ($CDCl_3$, 400 MHz): 8.34 (2H, d, *J* 7.8 Hz, Ar*H*), 7.91 (1H, t, *J* 7.8 Hz, Ar*H*), 7.46–7.33 (10H, m, Ar*H*), 5.86 (2H, t, *J* 9.3 Hz, NC*H*), 3.85 (2H, d of d, *J* 11.2, 9.3 Hz, SCH_2) and 3.36 (2H, d of d, *J* 11.2, 9.3 Hz, SCH_2). ^{13}C NMR ($CDCl_3$, 101 MHz): 150.3, 141.6, 137.4, 128.9, 127.9, 126.7, 123.8, 81.0, 39.7 and 1.03. IR (KBr, cm^{-1}): 3433 (m), 3134 (m), 2930 (w), 2907 (w), 1599 (s), 1582 (m), 1565 (w), 1491 (m), 1447 (s), 1429 (m), 1401 (m), 1313 (m), 1259 (w), 1212 (w), 1180 (w), 1155 (w), 1117 (w), 1079 (w), 1018 (s), 994 (m), 961 (w), 940 (s), 930 (m), 900 (w), 824 (m), 750 (s), 737 (m), 697 (s), 675 (w), 641 (m), 633 (m), 582 (w), 565 (w), 524 (w) and 424 (w). MS (ESI): *m/z* 825 (45%), 424 (M + Na, 35%) and 402 (M + H, 100%). Elem. Anal. Calcd for $C_{23}H_{19}N_3S_2$: C, 68.80; H, 4.77; N, 10.46. Found: C, 68.73; H, 4.82; N, 10.40.

2,6-Bis[(4*S*)-4-*tert*-butyl-4,5-dihydro-1,3-thiazol-2-yl]pyridine, L2

Prepared according to the procedure for **L1** using triethylamine (19.4 g, 191.7 mmol), *N*,*N*′-bis[(1*S*)-1-(hydroxymethyl)-2-*tert*-butyl]pyridine-2,6-dicarboxamide (1.4, 3.83 mmol) and phosphorus pentasulfide (2.59 g, 11.5 mmol) in dry toluene (150 mL). Yield = 0.62 g (45%). ^{1}H NMR ($CDCl_3$, 400 MHz): 8.19 (2H, d, *J* 7.7 Hz, Ar*H*), 7.83 (1H, t, *J* 7.7 Hz, Ar*H*), 4.47 (2H, d of d, *J* 9.5 Hz, SC*H*), 3.32 (2H, d of d, *J* 9.5 Hz, SC*H*) and 3.20 (2H, t, *J* 10. 8Hz, C*H*) and 1.08 (18H, s, *t*-Bu). ^{13}C NMR ($CDCl_3$, 101 MHz): 150.5, 137.0, 123.2, 88.2, 35.6, 32.7 and 26.8. IR (KBr, cm^{-1}): 3438 (m), 3136 (m), 2952 (s), 2865 (m), 1612 (s), 1567 (m), 1521 (w), 1474 (m), 1456 (m), 1392 (m), 1359 (m), 1325 (m), 1314 (w), 1288 (m), 1192 (w), 1147 (w), 1056 (m), 998 (s), 976 (w), 941 (s), 922 (m), 817 (m), 784 (w), 733 (m), 649 (m), 613 (w) and 567 (w). MS (ESI): *m/z* 745, 384 (45%, M + Na) and 362 (100%, M + H). Elem. Anal. Calcd for $C_{19}H_{27}N_3S_2$: C, 63.11; H, 7.53; N, 11.62. Found: C, 62.97; H, 7.48; N, 11.63.

2,6-Bis[(4*S*)-4-iso-propyl-4,5-dihydro-1,3-thiazol-2-yl]pyridine, L3

Prepared according to the procedure for **L1**, using triethylamine (8.83 g, 87.3 mmol), *N*,*N*′-bis[(1*S*)-1-(hydroxymethyl)-2-methylpropyl]pyridine-2,6-dicarboxamide (589 mg, 1.75 mmol) and phosphorus pentasulfide (1.18 g, 5.25 mmol) in dry toluene (100 mL). Yield = 130 mg (22%). ^{1}H NMR ($CDCl_3$, 400 MHz): 8.19 (2H, d, *J* 7.8 Hz, Ar*H*), 7.85 (1H, t, *J* 7.8 Hz, Ar*H*), 4.55 (2H, d of t, *J* 9.3, 6.3 Hz, C*H*), 3.39 (2H, d of d, *J* 9.2, 1.9 Hz, SC*H*) 3.12, (2H, d of d, *J* 9.2, 1.9 Hz, SC*H*), 2.14 (2H, sept., *J* 6.8 Hz, C*H*$(CH_3)_2$), 1.13 (6H, d, *J* 6.8 Hz, CH(C$H_3)_2$) and 1.05 (6H, d, *J* 6.8 Hz, CH(C$H_3)_2$). ^{13}C NMR ($CDCl_3$, 101 MHz): 150.5, 137.0, 123.0, 84.6, 34.1, 33.4, 19.7 and 19.9. IR (KBr, cm^{-1}): 3427 (m), 3134 (m), 2958 (m), 2867 (w), 1602 (s), 1566 (w), 1455 (m), 1401 (s), 1365 (w), 1308 (m), 1266 (w), 1228 (w), 1179 (w), 1024 (m), 993 (w), 957 (m), 941 (s), 886 (w), 824 (m), 741 (m), 647 (m), 589 (w) and 572 (w). MS (ESI): *m/z* 689, 356 (M + Na) and 334 (M + H). Elem. Anal. Calcd for $C_{17}H_{23}N_3S_2$: C, 61.22; H, 6.95; N, 12.60. Found: C, 61.14; H, 7.01; N, 12.55.

2,6-Bis(4,4-diphenyl-4,5-dihydro-1,3-thiazol-2-yl]pyridine, L4

Prepared according to the procedure for **L1** using *N*,*N*′-bis(2-hydroxy-1,1-diphenylethyl)pyridine-2,6-carboxamide (2.00 g, 3.59 mmol), phosphorus pentasulfide (2.42 g, 10.89) and triethylamine (18.20 g, 179.86 mmol) in dry toluene (150 mL). Yield = 1.06 g (53%). ^{1}H NMR ($CDCl_3$, 400 MHz): 8.41 (2H, d, $^3J_{HH}$ = 7.8 Hz, Ar*H*), 7.91 (1H, t, $^3J_{HH}$ = 7.8 Hz, Ar*H*), 7.65–7.45 (8H, m, Ar*H*), 7.44–7.21 (12H, m, Ar*H*) and 4.04 (4H, s, Ar*H*). ^{13}C NMR ($CDCl_3$, 101 MHz): 168.2, 150.7, 145.9, 137.3, 128.3, 127.2, 126.5, 123.5, 89.9 and 43.8. IR (KBr, cm^{-1}): 3392 (w), 3056 (w), 3025 (w), 2930 (w), 1683 (m), 1600 (m), 1495 (m), 1447 (s), 1316 (w), 1240 (w), 1156 (w), 1043 (m), 1029 (m), 1000 (w), 977 (w), 955 (w), 939 (m), 821 (w), 755 (m), 698 (s), 667 (w), 646 (w), 632 (w) and 609 (w). MS (ESI): *m/z* 554 ($[M + H]^+$, 100%).

2,6-Bis[4-(4-methylphenyl)-1,3-thiazol-2-yl]pyridine, L5

Pyridine-2,6-dithioamide (0.42 g, 2.13 mmol) and 2-bromo-4′-methylacetophenone (0.95 g, 4.47 mmol) were heated at reflux temperature in ethanol (40 mL) for 6 h. Upon cooling, water was added and the white precipitate collected *via* filtration and dried *in vacuo*. Yield = (0.586 mg, 65%). ^{1}H NMR ($CDCl_3$, 400 MHz): 8.39 (2H, d, *J* Hz, Ar*H*), 7.98 (1H, t, *J* Hz, Ar*H*), 7.93 (4H, d, *J* Hz, Ar*H*), 7.16 (2H, s, C*H*), 7.29 (4H, d, *J* Hz, Ar*H*), and 2.43 (6H, s, CH_3). ^{13}C NMR ($CDCl_3$, 101 MHz): 156.8, 151.0, 138.2, 131.6, 129.5, 126.3, 120.5, 115.0 and 21.4. IR (KBr, cm^{-1}): $\tilde{\nu}$ 3427 (m), 3115 (m), 3022 (w), 2912 (w), 1583 (w), 1567 (s), 1530 (w), 1507 (m), 1463 (s), 1441 (m), 1403 (m), 1310 (w), 1292 (m), 1246 (w), 1216 (w), 1200 (w), 1183 (w), 1149 (m), 1122 (w), 1056 (m), 1041 (w), 1015 (w), 995 (s), 944 (w), 902 (w), 851 (w), 842 (w), 818 (s), 791 (m), 762 (s), 740 (m), 688 (w), 675 (m), 643 (m), 575 (w), 492 (m) and 436 (w). MS (ESI): *m/z* 448 (100%, M + Na) and 426 (90%, M + H). Elem. Anal. Calcd for $C_{25}H_{19}N_3S_2$: C, 70.56; H, 4.50; N, 9.87. Found: C, 70.54; H, 4.40; N 9.75.

6-Bis[4-*tert*-butyl-1,3-thiazol-2-yl]pyridine, L6

Prepared according to the procedure for **L5** using pyridine-2,6-dithioamide (0.5 g, 2.53 mmol) and 1-bromopinacalone (1.23 g, 6.84 mmol) in ethanol (40 mL). Yield = (0.582 g, 64%). ^{1}H

NMR ($CDCl_3$, 400 MHz): 2.24 (2H, d, *J* Hz, Ar*H*), 7.88 (1H, t, *J* Hz, Ar*H*), 7.07 (2H, s, C*H*) and 1.44 (18H, s, *t*-Bu). ^{13}C NMR ($CDCl_3$, 101 MHz): 168.0, 167.5, 151.2, 137.8, 120.1, 113.2, 35.0 and 30.1. MS (ESI): *m*/*z* 380 (35%, M + Na) and 358 (100%, M + H). IR (KBr, cm^{-1}): $\tilde{\nu}$ 3427 (m), 3112 (m), 2961 (s), 2866 (w), 1584 (w), 1567 (m), 1505 (m), 1482 (w), 1457 (m), 1433 (m), 1401 (m), 1362 (m), 1298 (m), 1235 (m), 1205 (w), 1155 (w), 1109 (w), 1082 (w), 1047 (w), 1002 (s), 943 (w), 919 (w), 865 (w), 819 (s), 787 (m), 760 (m), 753 (w), 738 (m), 707 (w), 641 (m) and 581 (w). Elem. Anal. Calcd for $C_{19}H_{23}N_3S_2$: C, 63.83; H, 6.48; N, 11.75. Found: C, 63.78; H, 6.56; N, 11.65.

2,6-Bis[4-adamantyl-1,3-thiazol-2-yl]pyridine, L7

Prepared according to the procedure for **L5** using pyridine-2,6-dithioamide (0.5 g, 2.53 mmol) and 1-adamantyl bromomethylketone (1.37 g, 5.32 mmol) in ethanol (40 mL). Yield = (1.014 g, 78%). ^1H NMR ($CDCl_3$, 400 MHz): 8.30 (2H, d, *J* Hz, Ar*H*), 7.89 (1H, t, *J* Hz, Ar*H*), 7.02 (2H, s, C*H*), 2.16–2.11 (6H, s, C*H*), 2.10–2.06 (12H, m, CH_2), 1.85–1.81 (12H, m, CH_2). ^{13}C NMR ($CDCl_3$, 101 MHz): 168.2, 167.6, 151.0, 138.0, 120.4, 113.3, 42.2, 36.8, 28.6. IR (KBr, cm^{-1}): 3428 (m), 3117 (m), 2900 (s), 2846 (m), 1632 (w), 1580 (w), 1567 (m), 1504 (m), 1475 (m), 1450 (w), 1435 (m), 1401 (m), 1308 (w), 1277 (w), 1243 (w), 1172 (w), 1151 (w), 1104 (w), 1057 (m), 998 (s), 976 (w), 870 (w), 819 (m), 783 (w), 746 (w), 736 (m), 652 (w), 637 (w) and 577 (w). MS (ESI): *m*/*z* 536 (100%, M + Na) and 514 (97%, M + H). Elem. Anal. Calcd for $C_{31}H_{35}N_3S_2$: C, 72.47; H, 6.87; N, 8.18. Found: C, 72.35; H, 6.82; N, 8.15.

(4*R*,4′*R*)-2,2′-(2-Bromo-1,3-phenylene)bis(4-phenyl-4,5-dihydro-1,3-thiazole), L8

Prepared according to the procedure for **L1** using triethylamine (45.20 g, 446.68 mmol) 2-bromo-*N*,*N*′-bis[(1*R*)-2-hydroxy-1-phenylethyl]isophthalamide (4.32 g, 8.94 mmol) and phosphorus pentasulfide (6.03 g, 26.80 mmol) in dry toluene (300 mL). Yield = 0.32 g (8%). ^1H NMR ($CDCl_3$, 400 MHz): δ 7.63 (2H, d, $^3J_{HH}$ = 7.7 Hz, Ar*H*), 7.51–7.32 (11H, m, Ar*H*), 5.78 (2H, t, $^3J_{HH}$ = 9.5 Hz, C*H*), 3.95 (2H, dd, $^3J_{HH}$ = 9.0 Hz, $^2J_{HH}$ = 11.0 Hz, SC*H*) and 3.49 (2H, dd, $^3J_{HH}$ = 10.0 Hz, $^2J_{HH}$ = 10.8 Hz, SC*H*). ^{13}C NMR ($CDCl_3$, 101 MHz): δ 168.6, 141.3, 136.7, 131.5, 128.8, 127.9, 127.5, 126.8, 120.3, 80.4 and 42.4. IR (KBr, cm^{-1}): 3428 (m), 3185 (m), 3026 (w), 1619 (s), 1580 (m), 1492 (w), 1454 (m), 1436 (w), 1409 (m), 1344 (w), 1302 (w), 1272 (w), 1240 (w), 1221 (w), 1169 (m), 1050 (m), 1030 (m), 998 (m), 969 (w), 945 (m), 913 (m), 768 (m), 734 (m), 698 (s), 646 (m), 566 (w), 533 (m) and 494 (w). MS (ESI): *m*/*z* 479 ([M + H], 95%). Elem. Anal. Calcd for $C_{24}H_{19}BrN_2S_2$: C, 60.12; H, 3.99; N, 5.84. Found: C, 60.17; H, 3.89; N, 5.74.

(2,6-Bis[(4*R*)-4-phenyl-4,5-dihydro-1,3-thiazol-2-yl]pyridine) chromium(III) chloride, [Cr(L1)Cl_3]

2,6-Bis[(4*R*)-4-phenyl-4,5-dihydro-1,3-thiazol-2-yl]pyridine (**L1**) (400 mg, 0.97 mmol) and $CrCl_3$·3THF (373 mg, 0.97 mmol) were stirred together in THF (30 mL) for 16 h. After this time, the solution was passed through a glass filter and pentane was added to precipitate the product. Yield = 359 mg (64%). IR (KBr, cm^{-1}): 3433 (m), 3135 (w), 3062 (w), 3029 (w), 2943 (w), 1603 (w), 1533 (s), 1493 (m), 1453 (m), 1400 (m), 1323 (w), 1275 (w), 1239 (m), 1180 (s), 1131 (m), 1087 (w), 1018 (w), 959 (m), 908 (w), 842 (w), 820 (w), 759 (m), 720 (w), 695 (s), 643 (w), 590 (w), 524 (w) and 449 (w). MS (LSIMS): *m*/*z* 523 ($[M - Cl]^+$, 10%), 488 ($[M - 2Cl]^+$, 8%). Elem. Anal. Calcd for $C_{23}H_{19}Cl_3CrN_3S_2$: C, 49.34; H, 3.42; N, 7.50; S, 11.45. Found: C, 49.21; H, 3.48; N, 7.35; S, 11.34.

(2,6-Bis[(4*S*)-4-*tert*-butyl-4,5-dihydro-1,3-thiazol-2-yl]pyridine) chromium(III) chloride, [Cr(L2)Cl_3]

Prepared according to the procedure for [Cr(**L1**)Cl_3] using 2,6-bis[(4*S*)-4-*tert*-butyl-4,5-dihydro-1,3-thiazol-2-yl]pyridine (**L2**) (280 mg, 0.77 mmol) and $CrCl_3$·3THF (290 mg, 0.77 mmol) in THF (30 mL). Yield = 350 mg (87%). IR (KBr, cm^{-1}): 3424 (w), 3136 (w), 3064 (w), 3035 (w), 2964 (m), 2870 (w), 1607 (w), 1542 (m), 1531 (m), 1474 (m), 1422 (w), 1400 (m), 1368 (m), 1286 (w), 1235 (m), 1179 (s), 1128 (m), 1090 (w), 1042 (w), 980 (m), 911 (w), 826 (w), 753 (w), 691 (w), 627 (w), 590 (w), 444 (w) and 406 (w). MS (LSMIS): *m*/*z* 483 ($[M - Cl]^+$, 8%). Elem. Anal. Calcd for $C_{19}H_{27}Cl_3CrN_3S_2$: C, 43.89; H, 5.23; N, 8.08; S, 12.33. Found: C, 44.04; H, 5.35; N, 7.97; S, 12.18.

(2,6-Bis[4-(4-methylphenyl)-1,3-thiazol-2-yl]pyridine)chromium (III) chloride, [Cr(L5)Cl_3]

Prepared according to the procedure for [Cr(**L1**)Cl_3] using 2,6-bis[4-(4-methylphenyl)-1,3-thiazol-2-yl]pyridine (**L5**) (400 mg, 0.94 mmol), $CrCl_3$·3THF (350 mg, 0.94 mmol) in THF (40 mL) for 16 h. Yield = 472 mg (86%). IR (KBr, cm^{-1}): 3280 (m), 3115 (m), 2979 (m), 2908 (m), 1585 (w), 1567 (s), 1506 (m), 1462 (s), 1441 (m), 1407 (m), 1372 (w), 1341 (w), 1310 (w), 1292 (m), 1247 (w), 1216 (w), 1199 (w), 1183 (m), 1148 (m), 1122 (w), 1112 (w), 1056 (m), 1041 (m), 1013 (m), 995 (s), 972 (w), 944 (w), 920 (w), 902 (w), 853 (s), 818 (s), 791 (m), 763 (s), 740 (m), 687 (w), 675 (m), 643 (m), 575 (w), 492 (m) and 437 (w).

MS (LSIMS): *m*/*z* 547 ($[M - Cl]^+$, 3%). Elem. Anal. Calcd for $C_{25}H_{19}Cl_3CrN_3S_2$: C, 51.42; H, 3.28; N, 7.20; S, 10.98. Found: C, 51.51; H, 3.39; N, 7.14; S, 11.12.

(6-Bis[4-*tert*-butyl-1,3-thiazol-2-yl]pyridine)chromium(III) chloride, [Cr(L6)Cl_3]

Prepared according to the procedure for [Cr(**L1**)Cl_3] using 6-bis (4-*tert*-butyl-1,3-thiazol-2-yl)pyridine (**L6**) (0.48 g, 0.94 mmol) and chromium(III) chloride tetrahydrofuran complex (0.29 g, 0.94 mmol) in DCM (40 mL). Yield = 0.50 g (83%). IR (KBr, cm^{-1}): 3424 (w), 3125 (w), 2954 (m), 2869 (w), 1638 (w), 1603 (m), 1571 (m), 1494 (s), 1463 (m), 1399 (m), 1368 (m), 1300 (m), 1248 (s), 1202 (m), 1178 (s), 1111 (w), 1097 (w), 1031 (w), 941 (w), 894 (m), 810 (s), 777 (w), 762 (w), 742 (m), 726 (w), 712 (w), 674 (w), 583 (w), 552 (w) and 420 (w). MS (LSIMS): *m*/*z* 444 ($[M - 2Cl]^+$, 5%) and 358 ($M^+ - CrCl_3$, 15%). Elem.

Anal. Calcd for $C_{19}H_{23}Cl_3CrN_3S_2$: C, 44.23; H, 4.49; N, 8.15; S, 12.43. Found: C, 44.15; H, 4.41; N, 8.17; S, 12.53.

2,6-Bis[(4*S*)-4-*tert*-butyl-4,5-dihydro-1,3-thiazol-2-yl]pyridine iron(II) bromide, [Fe(L2)Br$_2$]

Prepared according to the procedure for [Cr(**L1**)Cl$_3$] using 2,6-bis[(4*S*)-4-*tert*-butyl-4,5-dihydro-1,3-thiazol-2-yl]pyridine (**L2**) (0.32 g, 0.89 mmol) and iron(II) bromide (0.19 g, 0.89 mmol) in THF (30 mL). Blue solid, Yield = 0.44 g (85%). Crystals suitable for X-ray analysis were obtained *via* a slow diffusion of diethyl vapour into a THF solution of the complex. ^{1}H NMR (CD_2Cl_2, 400 MHz): δ 57.53 (1H, s, Ar*H*), 54.35 (1H, br. s, NC*H*), 31.66 (2H, s, –C*H*$_2$–), 20.10 (2H, s, –C*H*$_2$–), −6.65 (18H, br. s, C(C*H*$_3$)$_3$) and −10.06 (1H, s, Ar*H*). IR (KBr, cm^{-1}): 3425 (w), 3139 (w), 2961 (s), 2868 (m), 1600 (w), 1551 (s), 1470 (m), 1434 (w), 1399 (m), 1368 (m), 1324 (w), 1287 (w), 1228 (m), 1172 (s), 1116 (s), 1092 (w), 1064 (w), 1027 (w), 1002 (m), 938 (w), 927 (w), 863 (w), 820 (m), 792 (w), 745 (w), 681 (w), 611 (w), 564 (w) and 518 (w). MS (LSMIS): *m*/*z* 577 (M^+, 30%), and 496 ([M − Br]$^+$, 100%). Elem. Anal. Calcd for $C_{19}H_{27}Br_2FeN_3S_2$: C, 39.53; H, 4.71; N, 7.28. Found: C, 39.60; H, 4.81; N 7.21.

6-Bis[4-*tert*-butyl-1,3-thiazol-2-yl]pyridine iron(II) bromide, [Fe(L6)Br$_2$]

Prepared according to the procedure for [Cr(**L1**)Cl$_3$] using 6-bis [4-*tert*-butyl-1,3-thiazol-2-yl]pyridine (**L6**) (0.52 g, 1.44 mmol) and iron(II) bromide (0.32 g, 1.44 mmol) in THF (50 mL). Red–brown solid. Yield = 0.66 g (80%). IR (KBr, cm^{-1}): 3417 (w), 3116 (m), 2958 (w), 1598 (m), 1567 (m), 1485 (s), 1460 (m), 1399 (s), 1366 (m), 1278 (w), 1240 (m), 1204 (w), 1176 (s), 1115 (w), 881 (w), 810 (m), 764 (m), 740 (w) and 581 (w). MS (LSIMS): *m*/*z* 492 ([M − Br]$^+$, 2%). Elem. Anal. Calcd for $C_{19}H_{23}Br_2FeN_3S_2$: C, 39.81; H, 4.04; N, 7.33; S, 11.19. Found: C, 39.94; H, 3.94; N, 7.29; S, 11.03. μ_{eff} = 5.2 BM.

(2,6-Bis[(4*R*)-4-phenyl-4,5-dihydro-1,3-thiazol-2-yl]pyridine) cobalt(II) chloride, [Co(L1)Cl$_2$]

2,6-Bis[(4*R*)-4-phenyl-4,5-dihydro-1,3-thiazol-2-yl]pyridine (**L1**) (450 mg, 1.12 mmol) in THF (50 mL) was added dropwise to cobalt(II) chloride (146 mg, 1.12 mmol) in THF. After stirring for 16 h, the precipitate was isolated *via* filtration, washed with pentane and dried *in vacuo*. Yield = (312 mg, 52%). IR (KBr, cm^{-1}): 3410 (m), 3181 (m), 3064 (w), 2940 (w), 1628 (m), 1601 (w), 1538 (s), 1493 (w), 1455 (m), 1431 (w), 1400 (m), 1349 (w), 1296 (w), 1277 (w), 1243 (m), 1175 (s), 1126 (s), 1087 (w), 1053 (w), 1028 (w), 1001 (w), 965 (m), 915 (m), 847 (w), 815 (w), 774 (m), 739 (w), 700 (s), 630 (w), 575 (w), 524 (w) and 430 (w). Elem. Anal. Calcd for $C_{23}H_{19}Cl_2CoN_3S_2$: C, 51.99; H, 3.60; N, 7.91; S, 12.07. Found: C, 51.87; H, 3.50; N, 7.84; S, 12.05.

(2,6-Bis[(4*S*)-4-*tert*-butyl-4,5-dihydro-1,3-thiazol-2-yl]pyridine) cobalt(II) chloride, [Co(L2)Cl$_2$]

Prepared according to the procedure for [Co(**L1**)Cl$_2$] using 2,6-bis[(4*S*)-4-*tert*-butyl-4,5-dihydro-1,3-thiazol-2-yl]pyridine (265 mg, 0.733 mmol) and cobalt(II) chloride (95.2 mg, 0.733 mmol) in THF (30 mL). In this case, the more soluble product was first precipitated by reducing the volume of the THF and adding pentane. Yield = 326 mg (66%). Crystals suitable for X-ray analysis were obtained by layering a dichloromethane solution of the complex with pentane. ^{1}H NMR (400 MHz, CD_2Cl_2): 52.2, −9.5, −12.9, −29.2, −40.3 and −48.0. IR (KBr, cm^{-1}): 3423 (m), 3142 (m), 3061 (w), 2955 (m), 2867 (w), 1629 (w), 1580 (s), 1466 (m), 1437 (w), 1400 (s), 1371 (m), 1322 (w), 1287 (w), 1230 (m), 1175 (s), 1138 (w), 1118 (m), 1090 (w), 1064 (m), 1029 (w), 998 (m), 935 (w), 859 (w), 832 (m), 754 (w), 614 (w) and 569 (w). MS (LSIMS): *m*/*z* 490 (M^+, 10%), 455 ([M − Cl]$^+$, 100%). Elem. Anal. Calcd for $C_{19}H_{27}Cl_2CoN_3S_2$: C, 46.44; H, 5.54; N, 8.55. Found: C, 46.57; H, 5.55; N, 8.52.

(2,6-Bis[(4*S*)-4-iso-propyl-4,5-dihydro-1,3-thiazol-2-yl]pyridine) cobalt(II) chloride, [Co(L3)Cl$_2$]

Prepared according to the procedure for [Co(**L1**)Cl$_2$] using 2,6-bis[(4*S*)-4-iso-propyl-4,5-dihydro-1,3-thiazol-2-yl]pyridine (**L3**) (0.70 g, 2.10 mmol) and cobalt(II) chloride (0.273 g, 2.10 mmol) in THF. In this case, the more soluble product was first precipitated by reducing the volume of the THF and adding pentane. Yield = (655 mg, 67%). Crystals suitable for X-ray analysis were grown by layering a dichloromethane solution of the complex with pentane. ^{1}H NMR (400 MHz, CD_2Cl_2): 75.7, −17.3, −20.0, −21.7, −28.2, −55.5 and −57.4. IR (KBr, cm^{-1}): 3423 (m), 3140 (m), 2956 (s), 2869 (m), 1562 (s), 1464 (m), 1437 (w), 1399 (m), 1369 (w), 1349 (w), 1281 (w), 1234 (m), 1172 (s), 1139 (w), 1118 (m), 1087 (w), 999 (w), 934 (w), 825 (m), 741 (m), 706 (w), 618 (w) and 569 (w). MS (LSIMS): *m*/*z* 462 ([M$^+$, 5%) and 427 ([M − Cl]$^+$, 100%). Elem. Anal. Calcd for $C_{17}H_{23}Cl_2CoN_3S_2$: C, 44.07; H, 5.00; N, 9.07. Found: C, 43.99; H, 5.05; N, 9.00. μ_{eff} = 3.8 BM.

(2,6-Bis[4-(4-methylphenyl)-1,3-thiazol-2-yl]pyridine)cobalt(II) chloride, [Co(L5)Cl$_2$]

Prepared according to the procedure for [Co(**L1**)Cl$_2$] using 2,6-bis[4-(4-methylphenyl)-1,3-thiazol-2-yl]pyridine (**L5**) (0.42 g, 0.97 mmol) and cobalt(II) chloride (0.13 g, 0.97 mmol) in THF (30 mL) for 16 h. Yield = 0.40 g (75%). IR (KBr, cm^{-1}): 3422 (s), 3063 (s), 1603 (m), 1568 (w), 1481 (s), 1253 (m), 1183 (s), 1138 (w), 1011 (w), 819 (s), 791 (w), 762 (w), 740 (w) and 530 (w). MS (LSIMS): *m*/*z* 519 ([M − Cl]$^+$, 5%) and 484 ([M − 2Cl]$^+$, 10%). Elem. Anal. Calcd for $C_{25}H_{19}Cl_2CoN_3S_2$: C, 54.06; H, 3.45; N, 7.57; S, 11.55. Found: C, 44.79; H, 2.49; N, 6.09; S, 10.26. μ_{eff} = 5.0 BM.

(6-Bis[4-*tert*-butyl-1,3-thiazol-2-yl]pyridine)cobalt(II) chloride, [Co(L6)Cl$_2$]

Prepared according to the procedure for [Co(**L1**)Cl$_2$] using 6-bis [4-*tert*-butyl-1,3-thiazol-2-yl]pyridine (**L6**) (0.40 g, 1.12 mmol), cobalt(II) chloride (0.15 g, 1.12 mmol) in THF (30 mL) for 16 hours. The lime pale green solid was collected *via* filtration and washed with ether (2 × 20 mL). Yield = 0.38 g (70%). IR

(KBr, cm^{-1}): 3418 (w), 3116 (m), 2963 (m), 2867 (w), 1598 (m), 1567 (m), 1493 (s), 1459 (m), 1435 (w), 1398 (m), 1366 (m), 1281 (w), 1243 (m), 1206 (w), 1176 (s), 1133 (w), 1115 (w), 1093 (w), 1020 (w), 881 (w), 810 (m), 765 (m), 742 (m), 709 (w), 673 (w), 582 (w) and 440 (w). MS (LSIMS): *m*/*z* 451 ($[M - Cl]^+$, 12%) and 416 ($[M - 2Cl]^+$, 2%). Elem. Anal. Calcd for $C_{19}H_{23}Cl_2CoN_3S_2$: C, 46.82; H, 4.76; N, 8.62; S, 13.16. Found: C, 46.95; H, 4.55; N, 8.57; S, 13.02. μ_{eff} = 4.7 BM.

(2,6-Bis[4-adamantyl-1,3-thiazol-2-yl]pyridine)cobalt(II) chloride, [Co(L7)Cl_2]

Prepared according to the procedure for [Co(**L1**)Cl_2] using 2,6-bis[4-adamantyl-1,3-thiazol-2-yl]pyridine (**L7**) (0.62 g, 1.21 mmol) and cobalt(II) chloride (0.16 g, 1.21 mmol) in THF. Yield = 0.54 g (69%). IR (KBr, cm^{-1}): 3418 (w), 3119 (m), 2905 (s), 2847 (m), 1599 (m), 1568 (w), 1488 (s), 1471 (s), 1400 (s), 1368 (w), 1342 (w), 1316 (w), 1296 (w), 1238 (w), 1183 (s), 1132 (w), 1053 (w), 880 (w), 811 (m), 753 (w), 740 (m), 712 (w), 577 (w) and 434 (w). MS (LSIMS): *m*/*z* 607 ([M − Cl], 18%), 570 ($[M - 2Cl]^+$, 3%). Elem. Anal. Calcd for $C_{31}H_{35}Cl_2CoN_3S_2$: C, 57.85; H, 5.48; N, 6.53; S, 9.96. Found: C, 57.79; H, 5.43; N, 6.37; S, 9.86. μ_{eff} = 4.7 BM.

(2,6-Bis[(4*R*)-4-phenyl-4,5-dihydro-1,3-thiazol-2-yl]pyridine) nickel(II) bromide, [Ni(L1)Br_2]

Prepared according to the procedure for [Co(**L1**)Cl_2] using 2,6-bis[(4*R*)-4-phenyl-4,5-dihydro-1,3-thiazol-2-yl]pyridine (0.40 g, 0.97 mmol) and 1,2-dimethoxyethane nickel(II) bromide (0.31 g, 0.97 mmol) in THF (30 mL). Yellow solid. Yield = 0.50 g (81%). IR (KBr, cm^{-1}): 3413 (s), 3100 (m), 3061 (m), 2944 (w), 1602 (m), 1538 (s), 1494 (w), 1455 (m), 1401 (m), 1347 (w), 1279 (w), 1243 (m), 1173 (s), 1126 (m), 1084 (w), 1031 (w), 966 (m), 913 (m), 873 (w), 846 (w), 823 (w), 771 (s), 698 (s), 631 (w), 524 (m) and 433 (w). MS (LSIMS): *m*/*z* 540 ($[M - Br]^+$, 30%) and 459 ($[M - 2Br]^+$, 35%). Elem. Anal. Calcd for $C_{23}H_{19}Br_2NiN_3S_2$: C, 44.55; H, 3.09; N, 6.78; S, 10.34. Found: C, 44.63; H, 3.17; N, 6.87; S, 10.45. μ_{eff} = 3.0 BM.

(2,6-Bis[(4*S*)-4-*tert*-butyl-4,5-dihydro-1,3-thiazol-2-yl]pyridine) nickel(II) bromide, [Ni(L2)Br_2]

Prepared according to the procedure for [Co(**L1**)Cl_2] using 2,6-bis[(4*S*)-4-*tert*-butyl-4,5-dihydro-1,3-thiazol-2-yl]pyridine (0.28 g, 0.77 mmol) and 1,2-dimethoxyethane nickel(II) bromide (0.24 g, 0.77 mmol) in THF (30 mL). Yellow solid. Yield = 0.40 g (90%).

IR (KBr, cm^{-1}): 3436 (w), 3139 (w), 2953 (m), 2869 (w), 1603 (w), 1544 (s), 1469 (m), 1436 (w), 1399 (m), 1367 (m), 1327 (w), 1289 (w), 1246 (w), 1229 (m), 1172 (s), 1120 (m), 1085 (w), 1055 (w), 1004 (m), 970 (w), 928 (w), 867 (m), 826 (m), 819 (m), 747 (m), 685 (w), 613 (w), 564 (w) and 442 (w). MS (LSIMS): *m*/*z* 500 ($[M - Br]^+$, 18%), 419 ($[M - 2Br]^+$, 20%). Elem. Anal. Calcd for $C_{19}H_{27}Br_2NiN_3S_2$: C, 39.34; H, 4.69; N, 7.24; S, 11.06. Found: C, 39.42; H, 4.67; N, 7.19; S, 10.92. μ_{eff} = 3.1 BM.

(2,6-Bis[4-(4-methylphenyl)-1,3-thiazol-2-yl]pyridine)nickel(II) bromide, [Ni(L5)Br_2]

Prepared according to the procedure for [Co(**L1**)Cl_2] using 2,6-bis[4-(4-methylphenyl)-1,3-thiazol-2-yl]pyridine (0.40 g, 0.94 mmol) and 1,2-dimethoxyethane nickel(II) bromide (0.29 g, 0.94 mmol) in THF (40 mL) for 16 h. Yield = 0.50 g (83%). IR (KBr, cm^{-1}): $\tilde{\nu}$ 3436 (m), 3063 (m), 3027 (m), 2918 (w), 1601 (m), 1567 (w), 1536 (w), 1492 (s), 1480 (s), 1469 (s), 1397 (m), 1378 (w), 1290 (w), 1250 (m), 1207 (w), 1179 (s), 1138 (m), 1065 (w), 1033 (w), 921 (w), 862 (m), 813 (m), 803 (m), 769 (m), 735 (m), 720 (w), 685 (w), 676 (w), 576 (w), 530 (w), 486 (w) and 438 (w). MS (LSIMS): *m*/*z* ($[M - Br]^+$, 20%), 483 ($[M - 2Br]^+$, 22%). Elem. Anal. Calcd for $C_{25}H_{19}Br_2NiN_3S_2$: C, 46.62; H, 2.97; N, 6.52; S, 9.96. Found: C, 46.55; H, 2.89; N, 6.47; S, 9.87. μ_{eff} = 2.8 BM.

(6-Bis[4-*tert*-butyl-1,3-thiazol-2-yl]pyridine nickel(II) bromide), [Ni(L6)Br_2]

Prepared according to the procedure for [Ni(**L5**)Br_2] using 6-bis [4-*tert*-butyl-1,3-thiazol-2-yl]pyridine (0.40 g, 1.12 mmol) and 1,2-dimethoxyethane nickel(II) bromide (0.35 g, 1.12 mmol) in THF (30 mL). Peach solid. Yield = 0.40 g (62%). IR (KBr, cm^{-1}): 3423 (w), 3121 (m), 2961 (m), 2904 (w), 2864 (w), 1600 (m), 1568 (m), 1492 (s), 1459 (m), 1440 (w), 1396 (w), 1365 (m), 1301 (w), 1286 (w), 1249 (s), 1205 (m), 1176 (s), 1133 (w), 1115 (m), 1091 (w), 1029 (w), 933 (w), 915 (w), 882 (m), 810 (s), 768 (m), 742 (m), 720 (w), 708 (w), 674 (w), 583 (w) and 443 (w). MS (LSIMS): *m*/*z* 496 ($[M - Br]^+$, 25%), 415 ($[M - 2Br]^+$, 50%). Elem. Anal. Calcd for $C_{19}H_{23}Br_2NiN_3S_2$: C, 39.62; H, 4.02; N, 7.29; S, 11.13. Found: C, 39.56; H, 4.00; N, 7.17; S, 11.06.

(2,6-Bis[(4*R*)-4-phenyl-4,5-dihydro-1,3-thiazol-2-yl]phenyl)nickel (II) bromide, [Ni(L8)Br]

To a solution of [Ni(COD)$_2$] (0.20 g, 0.72 mmol) in THF (30 mL) at −78 °C, a solution of ligand **L8** (0.25 g, 0.52 mmol) in THF (30 mL) was added dropwise. The experiment was performed in the absence of light. The reaction mixture was stirred for approximately 16 h, during which time it was allowed gradually to warm up to room temperature. After reducing the volume of THF to approximately 10 mL, pentane (30 mL) was added and a red solid precipitated. Yield = 0.21 g (74%). Single crystals suitable for X-ray analysis were grown by layering a dichloromethane solution of the complex with pentane. ^{1}H NMR ($CDCl_3$, 400 MHz): 7.35 (2H, d, $^3J_{HH}$ = 7.4 Hz, Ar*H*), 7.20–7.09 (6H, m, Ar*H*), 6.97 (2H, d, $^3J_{HH}$ = 7.5 Hz, Ar*H*), 6.77 (1H, Ar*H*, $^3J_{HH}$ = 7.5 Hz, Ar*H*), 5.78 (2H, d, $^3J_{HH}$ = 8.9 Hz, NC*H*), 3.05 (2H, dd, $^2J_{HH}$ = 10.9 Hz, $^3J_{HH}$ = 9.3 Hz, SCH_2) and 2.65 (2H, d, $^2J_{HH}$ = 10.9 Hz, SCH_2). ^{13}C NMR ($CDCl_3$, 101 MHz): 181.4, 177.2, 140.2, 137.9, 128.4, 127.7, 126.3, 125.6, 124.4, 72.1 and 42.4. IR (KBr, cm^{-1}): 3425 (w), 3129 (m), 3028 (w), 2985 (w), 1572 (m), 1494 (m), 1454 (m), 1400 (m), 1332 (m), 1289 (m), 1245 (m), 1184 (m), 1130 (s), 961 (w), 928 (w), 786 (w), 759 (m), 736 (w), 714 (w), 695 (s), 640 (w), 597 (w), 559 (w), 539 (w) and 470 (w). MS (LSIMS): *m*/*z* 538 (M^+, 8%), 457 ($[M - Br]^+$, 55%). Elem. Anal. Calcd for

Table 2 Crystal data, data collection and refinement parameters for the structures of **L1**, [Cr(**L2**)Cl_3], [Fe(**L1**)$_2$][$FeCl_4$], [Fe(**L2**)Br_2], [Fe(**L4**)Cl_2], [Co(**L2**)Cl_2], [Co(**L3**)Cl_2], [Co(**L5**)Cl_2] and [Ni(**L8**)Br]

Data	**L1**	[Cr(**L2**)Cl_3]	[Fe(**L1**)$_2$][$FeCl_4$]
Formula	$C_{23}H_{19}N_3S_2$	$C_{19}H_{27}Cl_3CrN_3S_2$	$[C_{46}H_{38}FeN_6S_4](FeCl_4)$
Solvent	—	CH_2Cl_2	MeCN
Formula weight	401.53	604.83	1097.62
Colour, habit	Colourless plates	Green plates	Dark purple platy needles
Crystal size/mm^3	0.40 × 0.39 × 0.07	0.10 × 0.08 × 0.03	0.27 × 0.05 × 0.01
Temperature/K	173	173	173
Crystal system	Monoclinic	Orthorhombic	Tetragonal
Space group	*I*2 (no. 5)	$P2_12_12_1$ (no. 19)	$P4_32_12$ (no. 96)
a/Å	5.5776(3)	10.16474(7)	13.3454(2)
b/Å	7.5976(4)	16.10208(9)	—
c/Å	22.5774(13)	16.90466(10)	26.6492(5)
β/°	92.097(5)	—	—
V/Å^3	956.11(9)	2766.84(3)	4746.24(12)
Z	2[b]	4	4[b]
D_c/g cm^{-3}	1.395	1.452	1.536
Radiation used	Mo-Kα	Cu-Kα	Mo-Kα
μ/mm^{-1}	0.293	9.365	1.056
2*θ* max/°	64	143	58
No. of unique reflns			
Measured (R_{int})	2970 (0.0431)	5359 (0.0585)	5782 (0.0977)
Obs, $\|F_o\| > 4\sigma(\|F_o\|)$	1730	4425	4149
No. of variables	128	307	310
R_1(obs), wR_2(all)[a]	0.0389, 0.0816	0.0280, 0.0603	0.0460, 0.0874

Data	[Fe(**L2**)Br_2]	[Fe(**L4**)Cl_2]	[Co(**L2**)Cl_2]
Formula	$C_{19}H_{27}Br_2FeN_3S_2$	$C_{35}H_{27}Cl_2FeN_3S_2$	$C_{19}H_{27}Cl_2CoN_3S_2$
Solvent	$^1/_3C_4H_8O$	—	$^2/_3CH_2Cl_2$
Formula weight	601.26	680.47	548.00
Colour, habit	Very dark blue needles	Brown blocks	Green blocks
Crystal size/mm^3	0.44 × 0.11 × 0.08	0.18 × 0.17 × 0.08	0.27 × 0.17 × 0.17
Temperature/K	173	173	173
Crystal system	Orthorhombic	Monoclinic	Orthorhombic
Space group	$C222_1$ (no. 20)	$P2_1/c$ (no. 14)	$P2_12_12$ (no. 18)
a/Å	15.5290(2)	12.66754(8)	12.12020(13)
b/Å	27.9269(4)	15.12678(8)	32.9663(4)
c/Å	17.3305(2)	16.74135(10)	9.29999(10)
β/°	—	109.6105(7)	—
V/Å^3	7515.84(17)	3021.89(3)	3715.89(7)
Z	12[c]	4	6[c]
D_c/g cm^{-3}	1.594	1.496	1.469
Radiation used	Mo-Kα	Cu-Kα	Cu-Kα
μ/mm^{-1}	3.972	7.162	10.406
2*θ* max/°	65	143	143
No. of unique reflns			
Measured (R_{int})	12 312 (0.0469)	5836 (0.0462)	7104 (0.0342)
Obs, $\|F_o\| > 4\sigma(\|F_o\|)$	8468	4542	6696
No. of variables	408	388	408
R_1(obs), wR_2(all)[a]	0.0293, 0.0722	0.0257, 0.0643	0.0312, 0.0836

Data	[Co(**L3**)Cl_2]	[Co(**L5**)Cl_2]	[Ni(**L8**)Br]
Formula	$C_{17}H_{23}Cl_2CoN_3S_2$	$C_{25}H_{19}Cl_2CoN_3S_2$	$C_{24}H_{19}BrN_2NiS_2$
Solvent	$^2/_3CH_2Cl_2$	—	CH_2Cl_2
Formula weight	519.95	555.38	623.08
Colour, habit	Green blocky needles	Dark green blocks	Colourless blocks
Crystal size/mm^3	0.20 × 0.12 × 0.12	0.24 × 0.13 × 0.10	0.16 × 0.16 × 0.08
Temperature/K	173	173	173
Crystal system	Orthorhombic	Monoclinic	Orthorhombic
Space group	$P2_12_12$ (no. 18)	$P2_1/n$ (no. 14)	$P2_12_12_1$ (no. 19)
a/Å	12.29660(6)	15.10734(17)	7.66033(7)
b/Å	32.40514(16)	10.71590(11)	12.99066(11)
c/Å	8.69965(5)	15.64386(17)	24.7438(2)
β/°	—	109.7307(12)	—
V/Å^3	3466.58(3)	2383.88(5)	2462.33(5)
Z	6[c]	4	4
D_c/g cm^{-3}	1.494	1.547	1.681
Radiation used	Cu-Kα	Cu-Kα	Mo-Kα
μ/mm^{-1}	11.123	9.497	2.815

Table 2 *(Contd.)*

Data	[Co(**L3**)Cl_2]	[Co(**L5**)Cl_2]	[Ni(**L8**)Br]
2θ max/°	143	143	65
No. of unique reflns			
Measured (R_{int})	6703 (0.0334)	4579 (0.0321)	8437 (0.0453)
Obs, $\|F_o\| > 4\sigma(\|F_o\|)$	6356	3679	7117
No. of variables	368	301	298
R_1(obs), wR_2(all)[a]	0.0216, 0.0557	0.0253, 0.0615	0.0310, 0.0797

[a] $R_1 = \Sigma\|\|F_o| - |F_c\|\|/\Sigma|F_o|$; w$R_2 = \{\Sigma[w(F_o^2 - F_c^2)^2]/\Sigma[w(F_o^2)^2]\}^{1/2}$; $w^{-1} = \sigma^2(F_o^2) + (aP)^2 + bP$. [b] The molecule has crystallographic C_2 symmetry [c] There are two crystallographically independent molecules in the asymmetric unit, one of which has crystallographic C_2 symmetry.

$C_{24}H_{19}BrN_2NiS_2$: C, 53.56; H, 3.56; N, 5.21. Found: C, 53.62; H, 3.56; N, 5.17.

General ethylene polymerisation procedure

The complex (10 μmol) in toluene (100 mL) was stirred under ethylene pressure for 5 min at room temperature. The co-catalyst (MAO, 500 eq.) was added and the reaction mixture was allowed to stir for 60 min. Ethylene was supplied on demand. At the end of the run, the excess pressure was vented and an accurately weighed quantity of GC-standard (2,2,4,4,6,8,8-heptamethylnonane) was added. Two aliquots of the solution (1 mL) were removed for GC analysis and the remaining solution quenched with MeOH (50 mL) followed by HCl (2M, 10 mL). Polyethylene that precipitated was collected by filtration and dried *in vacuo*.

General butadiene polymerisation procedure

The complex (10 μmol) in toluene (20 mL) was stirred under a pressure of butadiene (1 bar) for 15 min at room temperature. The co-catalyst (MAO, 500 eq.) was then added and the reaction mixture was allowed to stir for 30 min. Butadiene was supplied on demand. At the end of the run, the excess pressure was vented and an accurately weighed quantity of GC-standard (2,2,4,4,6,8,8-heptamethylnonane) was added. Two aliquots of the solution (1 mL) were removed for GC analysis and the remaining solution quenched with MeOH (50 mL) followed by HCl (2 M, 10 mL). The polymer that precipitated was collected by filtration and dried *in vacuo*. The polymer samples were analysed by GPC and by ^{13}C NMR spectroscopy (inverse-gated spectra were collected with a T_1 relaxation time of 15 s in order to allow all carbon nuclei to relax to their equilibrium state) to determine the microstructure of the polybutadiene.

X-ray crystallography

Table 2 provides a summary of the crystallographic data for the structures of **L1**, [Cr(**L2**)Cl_3], [Fe(**L1**)$_2$][$FeCl_4$], [Fe(**L2**)Br_2], [Fe(**L4**)Cl_2], [Co(**L2**)Cl_2], [Co(**L3**)Cl_2], [Co(**L5**)Cl_2] and [Ni(**L8**)Br]. Data were collected using Oxford Diffraction Xcalibur 3 (**L1**, [Fe(**L1**)$_2$][$FeCl_4$], [Fe(**L2**)Br_2] and [Ni(**L8**)Br]) and Xcalibur PX Ultra ([Cr(**L2**)Cl_3], [Fe(**L4**)Cl_2], [Co(**L2**)Cl_2], [Co(**L3**)Cl_2] and [Co(**L5**)Cl_2]) diffractometers, and the structures were refined based on F^2 using the SHELXTL and SHELX-97 program systems.[58] The absolute structures of **L1**, [Cr(**L2**)Cl_3], [Fe(**L1**)$_2$][$FeCl_4$], [Fe(**L2**)Br_2], [Co(**L2**)Cl_2], [Co(**L3**)Cl_2] and [Ni(**L8**)Br] were each determined by a combination of *R*-factor tests and by use of the Flack parameter. For **L1**, $R_1^+ = 0.0389$, $R_1^- = 0.0396$, $x^+ = +0.07(7)$, $x^- = +0.93(7)$; for [Cr(**L2**)Cl_3], $R_1^+ = 0.0280$, $R_1^- = 0.0782$, $x^+ = +0.000(5)$; for [Fe(**L1**)$_2$][$FeCl_4$], $R_1^+ = 0.0460$, $R_1^- = 0.0553$, $x^+ = +0.000(19)$; for [Fe(**L2**)Br_2], $R_1^+ = 0.0293$, $R_1^- = 0.0572$, $x^+ = +0.000(5)$, $x^- = +1.012(5)$; for [Co(**L2**)Cl_2], $R_1^+ = 0.0312$, $R_1^- = 0.1380$, $x^+ = +0.000(3)$; for [Co(**L3**)Cl_2], $R_1^+ = 0.0216$, $R_1^- = 0.1300$, $x^+ = +0.0000(19)$]; for [Ni(**L8**)Br], $R_1^+ = 0.0310$, $R_1^- = 0.0647$, $x^+ = +0.000(6)$. CCDC 859231 to 859239.

Acknowledgements

We are grateful to INEOS Technologies for financial support.

References

1 V. C. Gibson and G. A. Solan, *Top. Organomet. Chem.*, 2009, **26**, 107–158.
2 V. C. Gibson, C. Redshaw and G. A. Solan, *Chem. Rev.*, 2007, **107**, 1745–1776.
3 C. Bianchini, G. Giambastiani, I. Guerrero Rios, G. Mantovani, A. Meli and A. M. Segarra, *Coord. Chem. Rev.*, 2006, **250**, 1391–1418.
4 G. J. P. Britovsek, M. Bruce, V. C. Gibson, B. S. Kimberley, P. J. Maddox, S. Mastroianni, S. J. McTavish, C. Redshaw, G. A. Solan, S. Strömberg, A. J. P. White and D. J. Williams, *J. Am. Chem. Soc.*, 1999, **121**, 8728–8740.
5 G. J. P. Britovsek, V. C. Gibson, B. S. Kimberley, P. J. Maddox, S. J. McTavish, G. A. Solan, A. J. P. White and D. J. Williams, *Chem. Commun.*, 1998, 849–850.
6 G. J. P. Britovsek, S. Mastroianni, G. A. Solan, S. P. D. Baugh, C. Redshaw, V. C. Gibson, A. J. P. White, D. J. Williams and M. R. J. Elsegood, *Chem.–Eur. J.*, 2000, **6**, 2221–2231.
7 B. L. Small, M. Brookhart and A. M. A. Bennett, *J. Am. Chem. Soc.*, 1998, **120**, 4049–4050.
8 B. L. Small and M. Brookhart, *J. Am. Chem. Soc.*, 1998, **120**, 7143–7144.
9 B. A. Dorer, BP Chemicals Ltd., WO 00/47586, 2000.
10 D. Reardon, F. Conan, S. Gambarotta, G. Yap and Q. Wang, *J. Am. Chem. Soc.*, 1999, **121**, 9318–9325.
11 R. Schmidt, M. B. Welch, R. D. Knudsen, S. Gottfried and H. G. Alt, *J. Mol. Catal.*, 2004, **222**, 17–25.
12 M. A. Esteruelas, A. M. López, L. Méndez, M. Oliván and E. Onate, *Organometallics*, 2003, **22**, 395–406.
13 Y. Nakayama, K. Sogo, H. Yasuda and T. Shiono, *J. Polym. Sci., Part A: Polym. Chem.*, 2005, **43**, 3368–3375.
14 B. L. Small, M. J. Carney, D. M. Holman, C. E. O'Rourke and J. Halfen, *Macromolecules*, 2004, **37**, 4375–4386.
15 D. D. Devore, S. S. Feng, K. A. Frazier and J. T. Patton, Dow Chemicals, WO 00/69923, 2000.
16 T. M. Smit, A. K. Tomov, V. C. Gibson, A. J. P. White and D. J. Williams, *Inorg. Chem.*, 2004, **43**, 6511–6512.

17 T. M. Smit, A. Tomov, G. J. P. Britovsek, V. C. Gibson, A. J. P. White and D. J. Williams, *Catal. Sci. Technol.*, 2012, **2**, 643.
18 K. Tenza, M. J. Hanton and A. M. Z. Slawin, *Organometallics*, 2009, **28**, 4852–4867.
19 A. Tomov, J. J. Chirinos, D. J. Jones, R. J. Long and V. C. Gibson, *J. Am. Chem. Soc.*, 2005, **127**, 10166–10167.
20 A. Tomov, V. C. Gibson, G. J. P. Britovsek, R. J. Long, M. van Meurs, D. J. Jones, K. P. Tellmann and J. J. Chirinos, *Organometallics*, 2009, **28**, 7033–7040.
21 W. Zhang, W.-H. Sun, S. Zhang, J. Hou, K. Wedeking, S. Schultz, R. Fröhlich and H. Song, *Organometallics*, 2006, **25**, 1961–1969.
22 G. M. Lee, V. K. Appukuttan, H. Suh, C.-S. Ha and I. Kim, *Catal. Lett.*, 2011, **141**, 1608–1615.
23 R. Cariou, J. J. Chirinos, V. C. Gibson, G. Jacobsen, A. Tomov, G. J. P. Britovsek and A. J. P. White, *Dalton Trans.*, 2010, **39**, 9039–9045.
24 R. Cariou, J. J. Chirinos, V. C. Gibson, G. Jacobsen, A. Tomov and M. R. J. Elsegood, *Macromolecules*, 2009, **42**, 1443–1444.
25 S. K. H. Thiele and D. R. Wilson, *J. Macromol. Sci., Part C*, 2003, **43**, 581.
26 *Stereospecific Polymerization of Butadiene or Isoprene*, ed. R. Taube and G. Sylvester, VCH, Weinheim, Germany, 1996.
27 D. Gong, X. Jia, B. Wang, F. Wang, C. Zhang, X. Zhang, L. Jiang and X. Dong, *Inorg. Chim. Acta*, 2011, **373**, 47–53.
28 D. Gong, B. Wang, C. Bai, J. Bi, F. Wang, W. Dong, X. Zhang and L. Jiang, *Polymer*, 2009, **50**, 6259–6264.
29 D. Gong, B. Wang, H. Cai, X. Zhang and L. Jiang, *J. Organomet. Chem.*, 2011, **696**, 1584–1590.
30 Y. Nakayama, Y. Baba, H. Yasuda, K. Kawakita and N. Ueyama, *Macromolecules*, 2003, **36**, 7953–7958.
31 S. Tobisch, *Can. J. Chem.*, 2009, **87**, 1392–1405.
32 G. Desimoni, G. Faita and P. Quadrelli, *Chem. Rev.*, 2003, **103**, 3119–3154.
33 G. C. Hargarden and P. J. Guiry, *Chem. Rev.*, 2009, **109**, 2505–2550.
34 J.-i. Ito and H. Nishiyama, *Top. Organomet. Chem.*, 2011, **37**, 185–205.
35 C. Bolm, K. Weickhardt, M. Zehnder and T. Ranff, *Chem. Ber.*, 1991, **124**, 1173–1180.
36 K. Nomura, W. Sidokmai and Y. Imanishi, *Bull. Chem. Soc. Jpn.*, 2000, **73**, 599–605.
37 K. Nomura, S. Warit and Y. Imanishi, *Macromolecules*, 1999, **32**, 4732–4734.
38 M. A. Esteruelas, A. M. López, L. Méndez, M. Oliván and E. Onate, *New J. Chem.*, 2002, **26**, 1542–1544.
39 L. J. Ackerman, G. M. Diamond, K. A. Hall, J. M. Longmire and M. Micklatcher, Exxon-Mobil, WO 08/085657, 2008.
40 M. Redlich and M. M. Hossain, *Tetrahedron Lett.*, 2004, **45**, 8987–8990.
41 A. M. Tondreau, J. M. Darmon, B. M. Wile, S. K. Floyd, E. Lobkovsky and P. J. Chirik, *Organometallics*, 2009, **28**, 3928–3940.
42 H. G. Alt, H. A. Elagab and A. H. Al-Humydi, SABIC, WO 11/088990, 2011.
43 P. Le Maux, I. Abrunhosa, M. Berchel, G. Simonneaux, M. Gulea and S. Masson, *Tetrahedron: Asymmetry*, 2004, **15**, 2569.
44 J. Kuwabara, T. Namekawa, M.-A. Haga and T. Kanbara, *Dalton Trans.*, 2012, **41**, 44–46.
45 K. Okamoto, T. Kanbara, T. Yamamoto and A. Wada, *Organometallics*, 2006, **25**, 4026–4029.
46 I. Abrunhosa, M. Gulea, J. Levillain and S. Masson, *Tetrahedron: Asymmetry*, 2001, **12**, 2851–2859.
47 I. Abrunhosa, M. Gulea and S. Masson, *Synthesis*, 2004, 928–934.
48 T. Nishio, Y. Kodama and Y. Tsurumi, *Phosphorus, Sulfur Silicon Relat. Elem.*, 2005, **180**, 1449–1450.
49 S.-F. Lu, D.-M. Du, S.-W. Zhang and J. Xu, *Tetrahedron: Asymmetry*, 2004, **15**, 3433–3441.
50 A. W. Addison, T. N. Rao and C. G. Wahlgren, *J. Heterocycl. Chem.*, 1983, **20**, 1481–1484.
51 W. M. Reiff, N. E. Erickson and W. A. Baker, *Inorg. Chem.*, 1969, **8**, 2019–2021.
52 R. Boca, P. Baran, L. Dlhan, H. Fuess, W. Haase, F. Renz, W. Linert, I. Svoboda and R. Werner, *Inorg. Chim. Acta*, 1997, **260**, 129–136.
53 A. T. Baker, P. Singh and V. Vignevich, *Aust. J. Chem.*, 1991, **44**, 1041–1048.
54 J. P. Collman and E. T. Kittleman, *Inorg. Chem.*, 1962, **1**, 499–503.
55 F. C. Courchay, J. C. Sworen, I. Ghiviriga, K. A. Abboud and K. B. Wagener, *Organometallics*, 2006, **25**, 6074–6086.
56 A. T. Baker, P. Singh and V. Vignevich, *Aust. J. Chem.*, 1991, **44**, 1041–1048.
57 M. Murakata, H. Tsutsui and O. Hoshino, *Org. Lett.*, 2001, **3**, 299–302.
58 G. M. Sheldrick, *Acta Cryst.*, 2008, **A64**, 112–122.

